Works-in-Progress

Abstracts in this section pertain to papers submitted and accepted as Works-in-Progress at the 37th Annual Meeting of The Society of Nuclear Medicine, June 19–22, 1990 held at the Washington, DC Convention Center, Washington, DC.

Scientific Program Chairman: Peter T. Kirchner, MD

Bone Joint

Posterboard 1100

REGIONAL BONE MINERAL DENSITY CHANGES AFTER COLLES' FRACTURES: ASSESSMENT BY DUAL PHOTON ABSORPTIOMETRY J. Frohn, J. Jeibmann, J.M. Rueger, R. Inglis, E. Schaefer, A. Pannike, G. Hör. Department of Radiology, Division of Nuclear Medicine, and Department of Surgery, Division of Traumatology, Johann Wolfgang Goethe University Medical Center, Frankfurt/Main, FRG

We describe the preliminary results of an ongoing investigation to determine the profile of changes in bone mineral density at fracture sites during the normal healing process after cast removal. The investigation was cleared by the ethics board of the University of Frankfurt/Main.

The bone mineral density measurements were performed on a dual photon osteodensitometer (OSTEOTECH 300). In vivo precision for immediate repeat measurements was ± 0.01 grams/cm^2. We studied seven patients, five women and two men, with an age range of 25 to 71 yrs (median 48 yrs), who sustained a typical fracture of the distal radius and were treated with casts. All patients were right-handed. There were six fractures of the left radius, and one of the right radius. All patients were free of pain and their fractures were healing without complications. After the cast had been removed, the bone mineral density (BMD) was measured both at the fracture site and at the contralateral region. Follow-up studies were performed at monthly intervals over a period of six month.

The result of the investigation reveal that the BMD at the fracture site and the BMD of the corresponding skeletal region of the contralateral site were virtually constant during the course of the monitoring period.

This seems to indicate that during the healing process, without complication, mineralization is virtually complete at the time the cast is removed.

Cardiovascular Basic

Posterboard 1101

EVALUATION OF SIMULATED STRESS THALLIUM DATA BY BACK PROPAGATION NEURAL NETWORK (BPNN) ON PERSONAL COMPUTER. R. SHAH, LTC, MC, E. ACIO, CPT, MC, J. ANDERSON, COL, MC. Nuclear Medicine Service, Dept of Radiology, Walter Reed Army Medical Center, Washington, D.C. 20307

The Neural Networks are computer programs designed to learn associations. This abstract shows experience with a trained Back Propagation Neural Network (BPNN) to match input data to a diagnostic pattern. This study consists of data sets representing normal, fixed defect, and reversible defect patterns from simulated Stress Thallium studies in a single segment (septum). The BPNN has 4 input neurons, 12 hidden neurons, and 3 output neurons. The input neurons accept numerical values as average counts/pixel from the stress image (neuron #1) & delayed image (neuron #2), % clearance (neuron #3), and count modulation (neuron #4). The output neurons show matching pattern as normal (neuron #1), fixed defect (neuron #2), and reversible defect (neuron #3). The BPNN was trained with random presentation of 20 data sets to the input layer from each pattern (in all 60 data sets). On an IBM-AT compatible personal computer, the BPNN learned all patterns in 2.09 minutes. We evaluated the ability of this trained BPNN by presenting the same dataset in different random fashion without pattern identification. The following observations are made. (1) BPNN classified all 60 data sets correctly either as normal, fixed defect, or reversible defect in 15 secs. (2) The average probability of identification given to normal pattern is 98.3%, fixed defect 99.1% & reversible defect 98.9%. (3) This simulated study suggests that a BPNN, trained to recognize different imaging patterns could have clinical role.

Posterboard 1102

CHANGES IN MYOCARDIAL FATTY ACID AND PERFUSION IN CARDIOMYOPATHIC HAMSTERS. P.L. Pieri, R.A. Wilkinson, A.J. Fischman, R.J Callahan, M. Ahmad, and H.W.Strauss. Massachusetts General Hospital, Boston, MA.

The perfusion and fatty acid uptake in hamsters with dilated cardiomyopathy was assessed with a single IV injection of Tl-201 and ^{123}I beta methyl paraiodophenyl pentadecanoic acid, a fatty acid analog. Seven cardiomyopathic B10 14.6 syrian hamsters and five normal hamsters were evaluated 10 minutes after injection using dual photon imaging through a 2mm pinhole collimator for 10 minutes (80 kev mercury x-ray for Tl-201 and 159 kev photon for ^{123}I-FA). In all cardiomyopathic hamsters myocardial Tl-201 uptake increased while ^{123}I-FA remained unchanged. The ventricular function of each group was determined with gated blood blood imaging. The percentage of injected dose (% ID) within the myocardium was calculated for Tl-201 and ^{123}I-FA.

	CARDIOMYOPATHIC N=7	CONTROL N=5
%EF	15.44 ± 2.16	54.80 ± 4.47**
%ID TL	17.02 ± 2.51	9.69 ± 0.68*
%FA	5.44 ± 1.04	4.02 ± 0.43

*p<0.05; **p<0.01

In conclusion: A difference in myocardial uptake between ^{123}I-FA and Tl-201 in cardiomyopathic hamsters has been demostrated by in vivo imaging. A similar approach may be usefully used in patients with dilated cardiomypathies

Posterboard 1103

NOREPINEPHRINE-INDUCED LEFT VENTRICULAR DYSFUNCTION IN ANESTHETIZED VS CONSCIOUS-SEDATED DOGS. A. Movahed, S.L. Kearney, W.C. Reeves, and S.R. Jolly. East Carolina University, Greenville, NC.

High dose norepinephrine (NE) infusion to pentobarbital-anesthetized dogs significantly reduces left ventricular ejection fraction (LVEF) at 1 hour post-infusion. The aims of this study have been to determine whether similar injury occurs in chronic, morphine-sedated dogs and define the time course of recovery. Baseline equilibrium radionuclide angiography (RNA) was followed by infusion of NE, 5 μg/kg/min. for 90 min. Baseline LVEF was higher in conscious sedated vs. anesthetized dogs: 0.70±0.08 (mean±sd, n=7) vs. 0.54±0.06 (n=19, p<0.05). In 4 dogs, LVEF fell from 0.70±0.08, to 0.56±0.17, 0.40±0.23 and 0.33±0.25 at 30 min., 1 and 2 hours (hrs) post-NE infusion (All p<0.05). However, LVEF recovered to 0.65±0.15, 0.70±0.11, and 0.71±0.03 at 24, 48 hrs and one week respectively. In one dog, LVEF recovered slowly over one week. A second dog was still affected at 24 hrs. The remaining two dogs recovered to baseline LVEF over 24 hrs. Conclusions: 1. Pentobarbital anesthesia results in depressed baseline LVEF., 2. NE-induced reduction of LVEF is similar in conscious-sedated and anesthetized dogs., and 3. Depressed LVEF may reflect brief stunning rather than a long-term dilated myopathy.

Posterboard 1104

A KINETIC MODEL FOR C-11 ACETATE AS A TRACER FOR MYOCARDIAL OXIDATIVE METABOLISM. C.K. Ng, S.C. Huang, H.R. Schelbert, D.B. Buxton, UCLA School of Medicine, Los Angeles, CA.

The clearance of C-11 acetate (Ac) has been demonstrated to correlate well with myocardial oxygen consumption. The aim of this study was to formulate a compartmental model to describe the myocardial kinetic behavior of C-11 Ac. A bolus of 50 µCi C-14 Ac was administered to the aortic base of Langendorff perfused rat hearts which were then freeze-clamped at liquid N_2 temperature at either 5 min or 20 min. The distribution of tissue metabolites determined by phenylethylamine absorption of CO_2 and HPLC is shown below. Glutamate (~63%) was the major component of the amino acid (AA) fraction.

	n	CO_2%	TCA%	AA%
5 min	3	9.5±0.9	6.2±1.1	80.8±2.4
20 min	3	6.5±0.8	6.8±2.1	82.3±7.3

Tissue residue curves were measured externally in a second series of hearts given C-11 Ac. Analysis of these curves with the following model was consistent with the metabolite data.

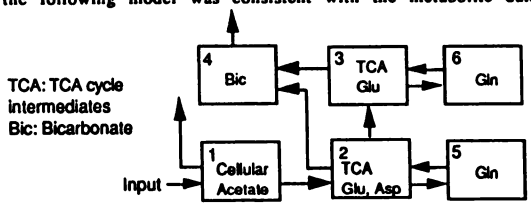

Posterboard 1105

PRELIMINARY EVALUATION OF MYOCARDIAL PERFUSION USING SPET AND PET. C. Landoni, G. Lucignani, G. Fragasso, M.C. Gilardi, C.Rossetti, F. Colombo, G. Rizzo, F. Zito, A. Conversano, G. Paganelli, S. Chierchia, F Fazio. ITBA-CNR, University of Milan, Institute H San Raffaele, Milan, Italy.

Myocardial rest perfusion studies were performed in patients with a clinical history of coronary artery disease (CAD) using both SPET and PET techniques. SPET studies were carried out using a rotating gamma camera Siemens Orbiter 90 min. after the i.v. administration of about 740 MBq (20 mCi) of Tc-99m-labeled methoxyisobutylisonitrile (MIBI). Images reconstruction was carried out without attenuation correction, transaxial resolution was 1.5 cm FWHM and slice thickness 3.2 mm. PET studies was performed with a ECAT 931/12 by CPS/Siemens 5 min. after the i.v. administration of about 370 MBq (10 mCi) of N-13-labeled ammonia (NH3). Images reconstruction was carried out with measured attenuation correction, transaxial resolution was 6.5 mm. FWHM and slice thickness was 6.7 mm. Three short axis slices, corresponding to the base, middle ventricle and periapical regions were examined for each patient. Average counts/pixel were calculated in four anatomical regions for each selected slice and data correlated. Preliminary data analysis indicates a good overall correlation between SPET/MIBI and PET/NH3, although differences possibly due to the effect of attenuation in the SPET study were observed in septal and lateral superior wall.

Cardiovascular Clinical

Posterboard 1106

FEASIBILITY OF SPECT PERFUSION IMAGING WITH TECHNETIUM 99m-TEBOROXIME: COMPARISON TO THALLIUM-201 AND QUANTITATIVE CORONARY ARTERIOGRAPHY. R.M. Fleming R.L. Kirkeeide, H. Taegtmeyer, D.B. Cassidy, Ajit Adyanthaya, J. Rodriguez-Bird, D. Jones, Y. Stuart, F. Velasco, R.A. Goldstein. The University of Texas Medical School at Houston, Houston, TX.

Technetium 99m-teboroxime (TEBO) is a new perfusion tracer that is highly extracted and rapidly cleared by the myocardium. To determine the utility of TEBO in the diagnosis of patients with suspected coronary artery disease, 18 patients underwent SPECT imaging with TEBO (20 mCi) at peak exercise and again 90 minutes later at rest. All patients had thallium stress SPECT studies and automated quantitative coronary arteriography (QCA) within 3 months of the TEBO studies without intervening revascularization or infarction. Images were reviewed by 2 investigators blinded to clinical data. Coronary lesions > 50 percent diameter narrowing by QCA were considered significant. Of 13 patients with disease, TEBO studies were abnormal in 12 and thallium in 11 (NS). In the remaining 5 patients without disease, the TEBO was normal in 4 and thallium in 3 (NS). When a lesion of > 75 percent area stenosis was used as the standard, the results were unchanged. There was concordance between the TEBO and thallium studies in 14/18. These results suggest that TEBO imaging has a sensitivity and specificity similar to that obtained with thallium. The rapid biologic half life allows studies to be completed within 2 hours which should aide patient throughput.

Posterboard 1107

CONTINUOUS SCINTIGRAPHIC BEDSIDE MONITORING OF RIGHT VENTRICULAR FUNCTION. L. Fridrich, D. Heute, G. Riccabona. Univ.-Klinik f. Nukl. Med. Innsbruck, Austria.

Recently, impaired right ventricular function (i. e. RVEF) has been evaluated as an additional risk factor for high mortality, especially if left ventricular function (i. e. LVEF) is decreased. Thus bedside monitoring of RVEF in critical ill pts. might be helpful for clinical management of these pts. Therefore RV- and LVEF as continuously assessed by a new miniaturized non imaging CsI-detector that was directly attached to the patients chest in connection with a PC, were compared with the EF-values computed from gamma-camera-studies after in vivo/in vitro-labelling of the patients red blood cells with 99mTc. Gamma-camera-studies for comparison with the detector were taken simultaneously for RVEF (ranging 38-71 EF %)+) in the optimal LAO-position (n=18). RVEF could be compared also during pharmacologic interventions (n=17).

Results: for LVEF the correlation was acceptable (R=0,79), SEE=9,7 EF %), however the correlation between camera detector RVEF was better (R=0,93, SEE=3,5 EF %); furthermore changes of RVEF during interventions (n=17) seen in camera studies were paralleled from RVEF-changes evaluated by the detector (R=0,88, SEE=3,1 EF %).

Conclusion: the new detector can be used for monitoring of RVEF, better than for LVEF as it can be placed more tightly over the right than over the left ventricle.

+) and consecutively for LVEF (ranging 22-77 EF %)

Posterboard 1108

PULMONARY Tc-99m ISONITRILE (MIBI) UPTAKE AS INDICATOR FOR STRESS INDUCED LV FAILURE IN CAD. F Mannting & MG Morgan, University Hospital, Uppsala, Sweden

A limitation of the newly introduced Tc-99m based myocardial perfusion imaging agents has been that they do not permit calculation of pulmonary uptake previously obtained from thallium 201 (Tl) imaging. Pulmonary Tl uptake is a recognized marker of stress induced LV dysfunction in patients with CAD. The purpose of this study was to determine whether pulmonary/myocardial (P/M) uptake ratios could be obtained with Tc-99m MIBI, and if so, do they correlate to Tl P/M ratios and myocardial perfusion abnormalities.

40 patients were investigated with Tc-99 MIBI. All patients performed maximal upright exercise and were imaged with SPECT. 22 were studied with MIBI and Tl imaging. P/M ratios were calculated in Tc-99 MIBI and Tl SPECT studies by published methods. The number of segments with abnormal perfusion (permanent & reversible) were totaled.

There was no difference ($p>0.05$) in achieved rate pressure product and Watt between the 2 stress tests. Correlation between pulmonary uptake of Tl and MIBI was $r=0.81$, $p<0.001$ for upper left lung uptake and $r=0.87$, $p<0.001$ for lower right lung uptake. A highly significant correlation to number of myocardial segments with abnormal perfusion was seen (n=40, $r=0.73$, $p<0.001$).

A pulmonary/myocardial ratio can indeed be obtained from Tc-99m MIBI studies - analogous to Tl ratios. MIBI

P/M ratios correlate to myocardial perfusion abnormalities. These findings dispel the original theory that P/M ratios can not be obtained from Tc-99m MIBI studies.

Posterboard 1109

TRANSIENT DILATATION OF LEFT VENTRICULAR CAVITY AFTER INTRAVENOUS DIPYRIDAMOLE ADMINISTRATION: AN INDICATOR OF SEVERE CORONARY ARTERY DISEASE. M. Tulchinsky and J.H. Murphy, Likoff Cardiovascular Institute, Hahnemann University, Philadelphia, PA.

We assessed the clinical significance of transient dilatation of the left ventricle (TDLV) during intravenous dipyridamole Tl-201 myocardial scintigraphy (IVDMS). The TDLV was defined as left ventricular enlargement on immediate post intravenous dipyridamole (IV-D) images that normalized or regressed significantly on the delayed images.

The left ventricular size was assessed visually by at least two experienced observers. The heart was divided into 10 segments and each of them was qualitatively graded from 0 to 3 (normal to absent activity). Redistribution score was calculated by subtracting the score of the delayed image from that of the initial image.

From 1/1/90 until 3/22/90 163 patients, age 62±10 (51% males), underwent IVDMS. Six patients (3.7%), with an age range of 58-80 years, demonstrated TDLV. All 6 patients underwent cardiac catheterization and all had extensive coronary disease (5 had three-vessel involvement and 1 patient had left main and left anterior descending arteries diseased). The initial image perfusion defect score was significantly higher in patients with TDLV than in the rest of the group (14.8±4.4 vs. 5±4.8, p<0.0001). In addition, the redistribution score was significantly higher in patients with TDLV (11.2±2.7 vs. 2.6±2.9).

The results of this work in progress suggest that TDLV is an infrequent finding on IVDMS; however, it is associated with extensive coronary disease. Further study of a larger population is needed to determine the prognostic implication of TDLV.

Posterboard 1110

SPECT VERSUS PLANAR LUNG/HEART RATIOS: CORRELATION WITH CARDIAC CATH LEFT VENTRICULAR END DIASTOLIC PRESSURE (LVEDP)
Margaret M. LaManna, M.D., FACC, Riyad Mohama, M.D., Kenneth M. Blasius, CNMT, Naipaul Rambaran, M.D., Frank J. Lumia, M.D., FACC, Vladir Maranhao, M.D., FACC
Deborah Heart and Lung Center, Browns Mills, NJ

Twenty-three patients mean age 57, underwent maximal exercise Thallium SPECT imaging with lung/heart (L/H) ratio calculation within 2 weeks of cardiac cath. Conventional L/H ratios are calculated based on an anterior planar image obtained prior to SPECT scanning. SPECT L/H ratio calculation was based on the 10th frame obtained in the anterior projection at approximately 56 degrees from the starting position. Two equal-size boxed regions of interest (ROIs), a 6 pixel sampling, were positioned. The heart ROI was placed at the highest pixel concentration of the myocardium and the lung ROI above the heart in the left lung area. The results and Thallium score (TS) were calculated: (Mean±SEM): LV ejection fraction 57.2±3.0, LV and diastolic pressure 15.1±1.7, systolic aortic pressure 131.0±5.9, diastolic aortic pressure 71.9±2.6, resting systolic pressure 140±4.1, resting diastolic pressure 85.6±2.2, exercise systolic pressure 167.2±5.9, exercise diastolic pressure 83.9±2.6, %maximal predicted heart rate 89.2±3.3, L/H ratio 0.41±0.02, TS 0.32±0.05. The correlation coefficient of L/H ratios with LVEDP was 0.73, $p < 0.01$, and with TS was 0.66, $p < 0.01$. SPECT L/H ratios provide an accurate non-invasive assessment of LVEDP. An anterior planar image is not required for calculation of L/H ratios.

Posterboard 1111

COMPUTER INTERPRETATION OF THALLIUM SPECT STUDIES BASED ON NEURAL NETWORK ANALYSIS. D.C. Wang, K.C. Karvelis. Henry Ford Hospital, Detroit, MI.

Interpretation of stress thallium studies is dependent on recognition of patterns characteristic for ischemia and infarction while allowing for anatomic variation. A class of artificial intelligence (AI) programs known as neural networks are well suited to pattern recognition and should allow a computer to provide a preliminary interpretation based on the stress and redistribution thallium images.

Neural networks are modeled after biological neurons and exhibit characteristics (learning, generalization, and abstraction) similar to the brain. The computer is trained to recognize patterns of normal perfusion, ischemia, and infarction by supplying patient images and their interpretation. The computer attempts to match its interpretation to the one provided, by modifying the internal parameters of the network. Training is repeated until a satisfactory level of accuracy is achieved. This approach differs from "expert system" AI programs in that it is not following a set of rules but rather a gestalt interpretation of the image based on previous training.

An initial trial of 50 selected stress and resting bull's-eye images were used for training. After 4000 evaluations of the 50 cases, the neural network is beginning to approximate the clinical impressions. Further work on the network parameters should yield a greater degree of correlation. It is doubtful that human interpretation will be supplanted by the computer, however neural network analysis may prove to be a useful adjunct to current myocardial perfusion evaluation and may have application to other studies.

Posterboard 1112

RECOGNITION OF VIABLE MYOCARDIUM WITH I-123 IODOPHENYLPENTADECANOIC ACID AFTER PRESUMED TRANSMURAL MYOCARDIAL INFARCTION. G. Murray, N. Schad, W. Ladd, R. Abben, S. Stagg, and C. Walker, Cardiovascular Institute of the South, Houma, LA; Institute of Radiological and Imaging Sciences, University of Siena, Italy.

We studied recognition of viable, jeopardized myocardium by I-123 iodophenylpentadecanoic acid (IPPA) imaging where myocardial infarction (MI) was presumed transmural based on (1) ECG Q-wave abnormalities and (2) akinesis or dyskinesis by 2-D echocardiography, first - pass radionuclide angiography (RNA), and cardiac catheterization.

17 pts. underwent resting myocardial imaging using 1 mCi IPPA i.v., a multicrystal gamma camera, and dynamic acquisition for 25 min. Regional clearing and accumulation rates were imaged for various time intervals according to the time/activity curves from the anterior, inferior and posterior left ventricular walls.

6 of 9 (66%) anterior MIs and 6 of 8 (75%) inferoposterior MIs, 12 of 17 (70%) total, showed metabolic viability. Exercise RNA showed worsening wall motion in all areas deemed viable by IPPA at rest. 4 pts. underwent revascularization (3 coronary artery bypass grafts, 1 angioplasty) resulting in improved wall motion. Myocardial biopsies during bypass confirmed IPPA results.

We conclude that resting IPPA imaging reliably identifies myocardial viability after MI presumed transmural by ECG, 2-D echocardiography, RNA, and cardiac catheterization.

Posterboard 1113

INTEROBSERVER AND INTRAOBSERVER REPRODUCIBILITY OF MYOCARDIAL SPECT Tc-99m SESTAMIBI PROCESSING. M.Miličinski, E.Henze, R.Weller, W.E. Adam, M. Porenta. Nucl. med., Univ.med.school, Ljubljana- Yugoslavia and Ulm- FRG

Quantitation of tomographic perfusion abnormalities is important for comparison of repeated studies either in follow up or in evaluation of success of medical, interventional or combined treatment in stable coronary disease or in evolving myocardial infarction. Modified Cedars program with polar coding was used for quantitation of myocardial SPECT Tc-99m Sestamibi studies. The extent of hypoperfused myocardium is given in percent of total myocardial area and the main coronary artery supply areas compared to the normal data base. The inter- and intraobserver variability of study processing in stable coronary artery disease was analysed and correlation (r) is as follows:

	LAD	RCA	LCX	TOTAL	No of studies
Interobs.r	0.94	0.88	0.76	0.90	40
Intraobs.r	0.95	0.76	0.24	0.87	26
Average defect (%)	18.9	10.4	8.4	14.1	66

We conclude that the reproducibility of quantitative evaluation of Sestamibi SPECT is very good. Careful interpretation of small perfusion defects is prudent for assessment of treatment results.

Endocrine

Posterboard 1114

VARIABLE SENSITIVITY OF TC/TL PARATHYROID IMAGING USING A SIMULTANEOUS DUAL ISOTOPE ACQUISITION TECHNIQUE. C.C. Chen, D. Sandrock, R.A. Wesley, M.J. Merino, J.A. Norton, R.D. Neumann, NIH, Bethesda, MD.

In an effort to improve test accuracy by minimizing motion artifacts during Tc99m/Tl-201 scintigraphy for hyperparathyroidism, we created a new simultaneous dual-isotope acquisition technique (EJNM 15: p411, 1989). We now report our initial results with this technique.

To date, 37 studies on 37 patients have been done; all technically satisfactory. Three studies were uninterpretable due to clinical Synthroid suppression of thyroid Tc uptake. Of the remaining 34 patients, 19 have since had surgery with resection of 31 abnormal parathyroids. Sixteen of these 19 patients had had one or more previous neck explorations prior to our scintigraphy. Scintigraphy was able to correctly locate only 13/31 lesions (42% sens): 6/9 adenomas (67% sens) in 9 patients and 7/22 hyperplastic glands (32% sens; p 2=.17) in 11 patients. One patient had an adenoma and several hyperplastic glands. Eight false positive foci were reported in 7 patients.

In comparison, our previous reports (JNM 5:860, 1988, and In press) of results using a sequential acquisition protocol in 104 patients with 127 lesions gave an approximate overall sensitivity of 38%: 42% for adenomas and 32% for hyperplastic glands (p 2=.33). Thus, our initial results with simultaneous dual-isotope acquisition suggest a modest improvement in detecting adenomas only.

Of additional interest, is that 6/19 patients were diagnosed as MEN-1. In this subgroup only 3/17 (18% sens) lesions (1 adenoma, 16 hyperplasias) were correctly identified by scintigraphy; while in the non-MEN-1 patients 10/14 (71% sens) lesions (8 adenomas, 6 hyperplasias) were correctly detected (p 2=.007). Possible reasons for these differences await further elucidation, but MEN-1 patients may constitute a subset of hyperparathyroid patients in whom Tc/Tl scintigraphy is particularly unreliable.

Gastroenterology

Posterboard 1115

SCINTIGRAPHIC FINDINGS IN ACUTE SCHISTOSOMIASIS: FOLLOW UP AFTER TREATMENT WITH OXAMNIQUINE. E. Orduña, F. Silva, C. García-Goyco, J. Vázquez-Selles, G. Vázquez. University of Puerto Rico, Medical Sciences Campus, San Juan, P.R.

Acute Schistosomiasis is a tropical parasitic disease caused by a blood fluke which inhabits the portal system of humans. A retrospective evaluation with liver and spleen scintigraphy (LSS) using Tc-99m sulfur colloid was done in 15 pediatric patients with the acute disease and successful treatment with oxamniquine. Extensive history, physical examination and complete laboratory work up was done, including the coprological tests by the Modified Ritchie technique. LSS was done before therapy, 7 months and 9 years after therapy. Initially the patients had abnormal cell counts and liver enzymes, with positive Circumoval test and a significant amount of ova in the feces. LSS showed hepatomegaly in 93% of the patients. Six months after therapy all laboratories were negative and the LSS now showed a reactive spleen in 78% of the cases; the hepatic image was unchanged. Long term follow up disclosed that the initial enlarged liver became normal (93%), however, 47% of the splenic images were still abnormal. The longitudinal scintigraphic changes in the liver were the expected for the natural history of the disease. The findings in the spleen suggest the persistence of an immunologic reaction with a continuous trigger, probably an antibody. These observations indicate that the LSS is more sensitive than the usual evaluation used in the follow up of these patients, and it could be used as a predictor of the severity of the immune response. At present we are working in a prospective study comparing the outcome of the LSS with serial immunologic tests in patients with the acute disease.

Posterboard 1116

SCINTIGRAPHIC EVALUATION OF GALLBLADDER FUNCTION FOLLOWING EXTRACORPOREAL SHOCK WAVE LITHOTRIPSY. K.P. Holdeman, C.H. Lorenz, L.G. Josephs, J.H. Arnold, J.A. Worrell. Vanderbilt University Hospital, Nashville, TN.

Extracorporeal shock wave lithotripsy (ESWL) is currently being used as non-surgical therapy for gallbladder (GB) stones. This study evaluates GB function pre- and post-lithotripsy using scintigraphic techniques.

Ten patients with symptomatic cholelithiasis had GB emptying studies prior to and 14 days following each ESWL treatment. Thirty minutes after IV administration of 5 mCi of Tc-99m mebrofenin, 10 ng/kg of CCK-OP was administered by infusion pump over 30 minutes. Computer images were acquired at 1 frame/5 minutes for 90 minutes. Time-activity curves were corrected for background and decay. Ultrasound was used to evaluate stone fragmentation and clearance.

Following ESWL, 2/10 patients were stone free. In this group, average ejection fraction at 20 min. from peak (EF20) was 5% ± 1.4% prior to and 51% ± 21% following ESWL. Residual fragments remained in 8/10 patients. Their average EF20 was 36% ± 22% prior to and 17% ± 15% following ESWL. These changes are not significantly different, and GB emptying halftime showed similar results.

ESWL does not alter GB function. Even in patients who became stone free, GB function was not improved. This suggests that cholelithiasis is related to GB dysfunction.

Posterboard 1117

CLNICAL EVALUATION OF TECHNETIUM-99m-GALACTOSYL SERUM ALBUMIN (Tc-GSA): A NEWLY DEVELOPED AGENT FOR LIVER FUNCTION STUDIES. S.K.Ha-Kawa[1], Y.Tanaka[1], Y. Kubota[1], M. Kudo[2], K. Ikekubo[2] and K. Torizuka[2].
1) Kansai Medical University, Moriguchi, 2)Kobe City General Hospital, Kobe, and 3)Fukui Medical School, Fukui, Japan.

Galactosyl serum albumin (GSA) labeled with technetium-99m, using DTPA as a bifunctional chelating agent, was evaluated in 5 normal volunteers and 53 patients with chronic liver diseases and compared with other liver function parameters. A single dose of GSA labeled with 185 MBq of technetium-99m was administered intravenously, and time-activity data were obtained from regions of interest over the precordium and liver. In normal cases administered 1 mg of GSA, the percent of the injected dose were 11.5 ± 1.1% (mean ± SD) in the blood, 58.2 ± 2.0% in the liver, and 6.6 ± 1.9% in the urine at 60 min after injection. The ratio of radioactivity at 30 min to that at 3 min in the heart, and the ratio of radioactivity in the liver to that in the heart and liver at 30 min, were calculated. These ratios showed siginificant correlations with the grading score of liver dysfunction and with the retention ratio of indocyanine green at 15 min in 33 cases administered 1 mg of GSA and 25 cases administered 3 mg of GSA.

These results suggested that Tc-GSA has characteristics for quantitating various degrees of liver dysfunction.

Neurology Clinical

Posterboard 1118

COMPARISON OF METHODS USED WITH 11C-RACLOPRIDE AND 11C-NMSP FOR DETERMINATION OF CENTRAL D2-DOPAMINE RECEPTOR CHARACTERISTICS. L. Eriksson, L. Farde, A.-L. Nordström and Chr. Halldin. Karolinska Institute, Stockholm, Sweden

The dopamine D2-receptor density in healthy subjects and in neuroleptic-naive patients with schizophrenia, has previously been determined by our group with positron emission tomography (PET) and 11C-raclopride . No significant differences in Bmax or Kd were found in the putamen and in the caudate nucleus between the two groups. These findings differ considerably from the results of Wong and colleagues, who have used PET and 11C-N-methyl-spiperone (11C-NMSP) . They found a 2-3-fold elevation in D2-dopamine receptor density in schizophrenic patients compared to healthy controls. In order to directly compare the two different techniques to determine the D2-dopamine receptor characteristics, we have performed initial experiments with both 11C-raclopride and 11C-NMSP in healthy subjects. These healthy subjects were also controls in a study with 11C-NMSP on acutely ill neuroleptic-naive schizophrenic patients. The experimental procedures for 11C-NMSP studies and the analyses of data were taken from the literature by Wong et al. We have so far analysed four healthy subjects and two neuroleptic-naive schizophrenic patients.

Table: Central D2-dopamine receptor densities (pmol/ml)

	11C-NMSP	11C-raclopride
Healthy subjects		
	24	28
	64	35
	42	33
	75	-

Schizophrenic patients
16
20

The Bmax values obtained with 11C-NMSP were higher for the healthy subjects than in the two schizophrenic subjects. These initial results do not confirm findings of Wong et al.

Posterboard 1119

BLOOD-BRAIN BARRIER DISRUPTION (BBBD) FOR CHEMOTHERAPY OF MALIGNANT GLIOMAS.
A. Singh, B.Belshe, M.K. Gumerlock, and R.A. Holmes. University of Missouri Hospital and Clinics, Columbia, MO.

Following surgical removal of malignant brain gliomas, local BBBD produced by intra-arterial hyperosmolar mannitol is used to administer chemotherapy. In 37 patients treated with BBBD-chemotherapy, their median survival increased to 22 months compared to 12-14 months in patients receiving conventional chemotherapy. Success and the degree of BBBD was assessed with I.V. Tc-99m DTPA injected immediately after BBBD. Of 232 scintigraphic studies, good disruption (2+ or 3+) was seen in 65%, with minimal disruption (1+) in 23%, and no apparent disruption in 12%. A disruption index (DI) defined as the ratio of count density from the area of BBBD but beyond the tumor margins to the count density from contralateral normal brain was determined. In patients with good disruption, the DI was 1.94 ± 0.44 compared to a DI of 1.42 ± 0.25 in patients with poor disruption. ($p < 0.0005$, Wilcoxan rank sum test) We conclude that the degree and extent of BBBD determines the effectiveness of chemotherapy and hence the improvement in patient survival.

Posterboard 1120

PET AND NEUROPSYCHOLOGIC CORRELATES OF AIDS
Van Gorp, W., Mandelkern, M., Gee, M., Evans, G., Flynn, F., Freeman, D., Paz, D., Dixon, W., Stern, C., Ropchan, J. and Blahd, W.

Introduction: The present study examined the relationship between cerebral metabolic and neuropsychologic (np) function in a consecutive series of AIDS patients enrolled without respect to dementia status.

Methods: 17 gay or bisexual males meeting CDC criteria for AIDS and 14 seronegative controls matched on age, gender, sexual orientation, handedness, and education were studied. Subjects ranged in age from 31 to 58 and no subject had evidence of past or present focal neurologic disease, head injury or substance abuse. Fasted subjects were studied with PET using ^{18}2-fluro 2-deoxyglucose in a resting state paradigm. Metabolic values were normalized by subjects' whole brain metabolic activity.

Results: T-tests revealed significant differences in metabolic activity between AIDS subjects and controls in the frontal, temporal and subcortical regions. Discriminant function analysis also suggested that these three regions contributed best toward group separation, predicting 81% of the AIDS' and 86% of the controls' group membership correctly. Though several np measures were significantly different between groups, the correlations between the np and resting state metabolic measures were low.

Discussion: These data suggest that HIV affects cerebral metabolism in a symptomatic HIV infected group unselected for dementia status. Frontal, temporal and subcortical regions appear differentially affected.

Posterboard 1121

CEREBELLAR VASOREACTIVITY IN VERTEBRO-BASILAIR INSUFFICIENCY : A DIAGNOSTIC TEST ?
F. Delecluse, Ph.Voordecker, S. Motte*, J.P. Wautrecht, and J.P. Dereume*. Departements de Neurologie et de Chirurgie Vasculaire*, Hôpital Erasme 808 Route de Lennik, 1070 Bruxelles, Belgium.

The various cerebellar imaging techniques (CT-scan, NMR) as well as the electrophysiological brainstem tests (ENG, Evoked Potentials) can do little to confirm the difficult clinical diagnosis of vertebrobasilar insufficiency (VBI). We decided to study cerebellar vascular function by evaluating the cerebellar vasodilatation response to the cerebral vasodilator Diamox (acetazolamide), by means of the 133 Xenon inhalation technique and a dedicated single photon emission computerized tomograph, the Tomomatic 564 (Medimatic, Copenhagen, Denmark). We prospectively studied 17 consecutive patients (mean age= 62.7 +/- 10.8 yrs) who fulfilled the following criteria : a) certain VBI, b) normal CT-scan, c) no other disease of the SNC. Their data was compared to that of a group of 17 normal controls of similar age (61.9 +/- 13.8 yrs). As opposed to the controls, these 17 patients showed highly significant ($p<0.01$) abnormalities of cerebellar perfusion, in three types of pattern :

a) normal resting flows, but significant asymmetry ◊ 5 ml/100/ml) of the Diamox-induced flow increases,
b) resting flow asymmetry>5 ml/100g/ml between the two cerebellar hemispheres, with a parallel ipsilateral decrease of the vasodilatatory response,
c) resting flow asymmetry>5 ml/100g/ml between the two cerebellar hemispheres, with a paradoxical flow decrease after Diamox, indicating a vascular steal.

We therefore suggest that 133 Xenon SPECT and the Diamox test can be used in the diagnosis of VBI.

Neurology Basic

Posterboard 1122

REGIONAL CEREBRAL HEMATOCRIT, MEAN TRANSIT TIME, BLOOD VOLUME AND BLOOD FLOW IN CANINE ACUTE STROKE MODEL.
G.D. Arora, J.K. Payne, J.L. Lowe, P.V. Kulkarni, M.D. Devous, Sr. University of Texas Southwestern Medical Center, Dallas, TX

Regional cerebral blood flow (rCBF), blood volume (rCBV) and hematocrit (rCHCT) were measured in infarct center (IC), peri-infarct (PI) and normal contralateral zones (NCZ) in a canine model (N=5). Permanent middle cerebral artery ischemia was produced by intravascular delivery of microfibrillar collagen. After 8 hours, brain was rapidly removed and frozen in liquid nitrogen. RCBF was estimated using tracer microspheres, and rCBV was measured using both RBC (Tc-99m-RBC) and plasma (I-125-HSA) radiotracers. For each dog rCBF, rCBV, regional transit time (rT), rCBF/rCBV and rCHCT data from 50 brain regions were digitized into image format. Values from regions of interest representing IC, PI and NCZ appeared as distinct subgroups in plots of rCBF vs rCBV, rT (rCBV/rCBF) vs rCBF, and rT vs rCHCT. When compared to NCZ, rCBV was decreased by 42% in metabolically depressed IC, but increased by 30% in PI, demonstrating misery perfusion. RT increased by 1200% and 267% in IC and PI respectively as compared to NCZs. When compared to normal, IC had the highest rT (1.17±0.23 min, $p<.001$) and rCHCT (0.40±0.06). RCHCT in PI and NCZ were not statistically different. In all NCZ, rCBF/rCBV ratio was >7 min-1 (IC values were 0.91± 0.4 min-1, $p<.002$) and rT was <.07 min ($p<.001$). RT and rCHCT in IC and PI are readily measured by SPECT techniques.

Posterboard 1123

Imaging Serotonin-S2 receptors in humans with PET and the selective S2 antagonist [^{18}F]-altanserine.

B. Sadzot, C. Lemaire, R. Cantineau, E. Salmon, A. Plenevaux, G. Franck, M. Guillaume
Cyclotron Research Center and Department of Neurology, University of Liège, B30, 4000 Liège Belgium

Serotonin-2 receptors are thought to play a role in various neurodegenerative and affective disorders including Alzheimer's disease and depression. Radioligands that are available to label these receptors in vivo with PET are either non specific or display a low total/non specific (NS) binding ratio.

Altanserine is a high affinity S2 receptor antagonist that is 30 fold less potent towards α1 receptors as compared with S2. [18F]-altanserine was synthesized as previously described by nucleophilic substitution (1). The radiosynthesis has recently been improved by the development of a remote control system and a new HPLC purification.

Preliminary animal studies have indicated that high total/NS binding ratios are reached in vivo with [18F]-altanserine.

A normal volunteer was administered 6.2 mCi of high SA (1368 Ci/mmol) [18F]-altanserine. Brain images were obtained with a NeuroEcat PET scanner. Imaging planes passed through the cerebellum (CB, plane 1), the thalamus (TH), the caudate (CA) and the cortex (plane 2). The ligand readily crossed the BBB. The cerebral activity peaked at 20 min post-injection at ± 3 % of the injected dose/l. A rapid washout was observed from the CB, the TH and the CA, structures with few or no S2 receptors, while the activity was retained in the cerebral cortex. The retention of [18F]-altanserine is indicative of its selectivity. The frontal/CB binding ratio plateaued at ± 2.6 after 60 min.

These preliminary results indicate that [18F]-altanserine is a suitable ligand for imaging serotonin-S2 receptors in vivo with PET and may be preferable to other radioligands for imaging serotonin receptors because of its selectivity.

(1) Lemaire C. et al, J. Label. Comp. Radiopharm., 1988, 26, 336

Posterboard 1124

EFFECT OF AGE ON CEREBRAL METABOLIC RATE OF GLUCOSE. J.M. Lorenz, J.T. Metz, M.D. Cooper. The University of Chicago, Chicago, Il.

In a preliminary study of the effects of aging on regional cerebral metabolic rate of glucose (CMRglu), we retrospectively examined data obtained in previous studies.

All subjects were studied with a PETT VI and 18-F-2FDG. Seven regions of interest were examined bilaterally. All subjects were physically healthy and psychologically normal and were arranged into three groups: 6 males, aged 20-30, who performed a visual verbal memory recall task during the period of FDG equilibration (young memory task group--YMT); 6 males, aged 20-30, who performed a sensory-motor attention task (young sensory-motor group--YSM); 2 males and 2 females, aged 69-73, who performed an oral verbal memory recall task (elderly memory task group--EMT).

Global CMRglu averaged 9.89 (S.D. ± 1.08) mg/100g/min in YMT, 9.37 (±1.20) in YSM, and 6.40 (± 1.56) in EMT. The EMT group was significantly lower in CMRglu than either of the other groups ($p<.02$); the YMT and YSM groups did not differ from each other. The decrease in CMRglu in the EMT group was widespread, with the frontal, parietal and occipital lobes showing the largest effect (up to 40% less than the YMT group), and the thalamus showing the smallest effect (26% less than YMT).

Although the groups were not exactly matched, the results indicate that the effects of age on CMRglu are much greater than those attributable to task or gender. The influence of age on CMRglu must, therefore, be considered in evaluating possible pathology in individual subjects and warrants further systematic study.

Oncology (Non-antibody)

Posterboard 1125

VALIDATION OF A NEW PROTOCOL FOR THE TREATMENT OF WELL DIFFERENTIATED THYROID CARCINOMA: PRELIMINARY REPORT. F. Silva, E. Vázquez-Quintana, F. Aguiló, J. Vázquez-Selles and J. Negrón. University of Puerto Rico, Medical Sciences Campus, San Juan, P.R.

The importance of disease control in well differentiated thyroid cancer is well established. Treatment with I-131 iodine requires patient hospitalization. In an attempt to reduce the cost of treatment, a control study was started on 1981. A total of 45 patients with a mean age of 42 have been included in the protocol. Patients were randomized in two groups for treatment: ambulatory and hospitalized. All patients had total thyroidectomy and a whole body scan with I-131 iodine was performed. The patients were then classified in three groups, according to the extension of the disease. A preestablished dose, ranging from 50 mCi to 200 mCi was administered according to the classification of the disease. Ambulatory treatment required alternate day administration of 25-29 mCi, until the total calculated dose was completed. Annual follow up was done with whole body studies and thyroglobulin determinations. Preliminary evaluation of the data reveals no significant difference in disease control in both groups. There was no statistical difference in cure rate, recurrence, morbidity and mortality. We believe this preliminary data is highly encouraging and favors our protocol for ambulatory treatment. Further follow up is needed to evaluate the long term effects as well as the patient outcome with this therapeutic modality.

Posterboard 1126

CARBON-11 LABELED THYMIDINE (TdR) ACCUMULATION IN PRIMARY AND METASTATIC BRAIN TUMORS: PRELIMINARY CLINICAL TRIALS USING POSITRON EMISSION TOMOGRAPHY. P.S. Conti, S.A. Grossman, A.A. Wilson, D.F. Wong, J. Hilton, J. H. Anderson, R.F. Dannals, J. Zinreich, E.E. Camargo and H.N. Wagner, Jr. The Johns Hopkins Medical Institutions, Baltimore, MD.

The measurement of DNA synthesis can be used as an index of cellular proliferation rate and to assess tumor growth and response to therapy. Using C-14 and C-11-methyl-thymidine we have correlated the accumulation of C-14 TdR in tumor DNA with tumor uptake of C-11 TdR in a canine glioma model using standard biochemical assays, quantitative autoradiography and PET. In preliminary clinical trials, patients with primary or metastatic brain tumors have been studied with 20 mCi of C-11 TdR and PET following assessment with computed tomography (CT) and/or gadolinium enhanced magnetic resonance imaging (MRI). Three patients with high grade gliomas have been studied, including two with grade IV cystic astrocytomas which were well visualized at 15 minutes. The third patient demonstrated abnormal accumulation of tracer in residual tumor following surgical debulking. A fourth patient, previously treated with radiation therapy for a small cell carcinoma of the ethmoid sinus, presented with an intracranial mass lesion within the radiation port which was thought to represent radiation necrosis or metastatic disease by CT and gadolinium MRI. C-11 TdR accumulation was observed in this lesion, correlating with the presence of metastatic tumor at surgery. These preliminary trials demonstrate that brain tumor imaging with PET and C-11 TdR may serve as a means for in vivo assessment of cellular proliferation.

Posterboard 1127

DISTRIBUTION OF 111-In LABELED LYMPHOCYTES AFTER IL-2 ADMINISTRATION. C. Hoh, G. Sarna, E. Jacobs, D. Marciano, R. Hawkins, UCLA School of Medicine, Los Angeles, CA.

We have studied 2 patients with 111-In labeled lymphocytes after stimulation with Interleukin-2 (IL-2) to determine the distribution of these lymphocytes in the blood, plasma, and lymphatic system, and to confirm that the decrease in peripheral lymphocytes count is due to the migration of lymphocytes into the peripheral lymphatic system. Patients were injected with 0.5 mCi 111-In lymphocytes iv (which were obtained from the cannulated thoracic duct, and prepared as described by Thakur[1]); peripheral venous blood and the lymphatic fluid from the cannulated thoracic duct were sampled up to 46 hrs. post injection. IL-2 was given intravenously at 25 hrs post lymphocyte injection. Planar images were obtained at 3, 6, 24, 38, and 48 hrs and SPECT images at 32 and 48 hrs with a Siemens Orbiter camera. Lymphocyte, plasma, and blood activity curves demonstate a decrease in lymphocyte activity in both the peripheral blood and lymphatic fluid starting approximately 2-6 hrs post IL-2 injection. The images demonstrated progressive increase in lymphocyte activity in the peripheral lymph nodes believed to be involved with the primary malignancy.

1. Thakur M. L. et al, J. of Nucl. Med. 18:1014-1021,1977

Posterboard 1128

POSITRON EMISSION TOMOGRAPHIC IMAGING WITH F-18-DEOXYGLUCOSE OF MALIGNANT PLEURAL MESOTHELIOMA

M.V. Knopp, L.G. Strauss, U. Haberkorn, A. Dimitrakopoulou, H. Menke, H.G. Bauer, J. Doll, G. van Kaick

German Cancer Research Center, Heidelberg, West-Germany.

The evaluation of pleural mesothelioma with conventional techniques including CT and MRI remains limited especially for evaluation of therapy response. We use PET with a metabolically active compound, F-18-labeled deoxyglucose (FDG), to detect increased uptake in malignant mesothelioma and to evaluate its changes during follow up. We performed endpoint measurements 50 min post injection of 12 mCi (444 MBq) FDG iv. and acquired transmission scans of 5 min and emission scans of 15 min. Each patient was studied by CT prior to the PET exam. Tracer uptake concentrations were calculated by a ROI- technique, standardized for injected dose and body volume and expressed as standardized uptake values (SUV). We already performed 25 PET studies of patients with confirmed pleural mesothelioma including

10 studies as follow up. Surgical resection of the mesothelioma was performed in five patients and the areas of high FDG uptake were confirmed to be malignant mesothelioma. We found different uptake patterns between mesothelioma of the pleura and pleuritis. We can summarize in our initial evaluation, that

- PET enables metabolic oriented imaging of pleural mesothelioma with high contrast
- the metabolic activity can be used to monitor promptly the therapy response
- PET permits differentiation of scar tissue and tumor recurrence

Posterboard 1129

PET IN PATIENTS WITH ADVANCED HEAD AND NECK CANCER: CHEMOTHERAPY MANAGEMENT USING F-18-DEOXYGLUCOSE. U. Haberkorn, L.G. Strauss, M. Knopp, A. Dimitrakopoulou, C. Reisser, E. Seiffert, J. Doll, G. van Kaick. German Cancer Research Center, Heidelberg, Germany.

Combinations of cisplatinum and 5-FU for the treatment of advanced head and neck cancer result in high remission rates. While CT and MR give morphologic information about the tumor size and infiltration, PET with F-18-Deoxyglucose (FDG) provides quantitative data about the tumor metabolism. In 10 patients with histological proved tumors of the oro- or hypopharynx PET studies with 12mCi intravenously injected FDG were done prior and after the first chemotherapeutic cycle. Tumor and/or lymph node volumes were determined from CT slices and the tumor growth rate was calculated assuming an exponential function. After standardization of the PET images for the body weight and the injected dose, a quantitative evaluation was done using a region of interest technique. FDG data were available for 5 tumors and 9 lymph nodes, volumetric data for 4 tumors and 7 lymph nodes. In one case there was an increase in FDG accumulation, whereas 7 lesions showed a decrease. Six lesions remained without change of the metabolism. We found that multiple lymph nodes in the same patient can show a different metabolic activity and also a different response to therapy. In general tumors were more sensitive to therapy. There was a high correlation between the changes in FDG uptake and tumor growth rate (r=0,9). We conclude from our results that PET should be used for the therapy management and the evaluation of therapeutic effects in patients with systemic chemotherapy.

Immunology (Antibody)

Posterboard 1130

A TRIAL OF Tc-99m LABELED MONOCLONAL ANTIBODY FOR IMAGING MELANOMA IN PATIENTS BEFORE LYMPHADENECTOMY. M.J. Blend, A. Malpani, C. Bekerman, J. Golick, Michael Reese Hospital, Chicago, IL: S. Ronan and T.K. Das Gupta, University of Illinois School of Medicine, Chicago, IL: K. Sullivan, D. Salk and P. Abrams, NeoRx Corporation, Seattle, WA.

The purpose of this investigation was to evaluate the detection rate of distant metastasis in melanoma patients (pts) with lymph node involvement limited to the drainage region of the primary lesion as determined by physical and radiological exams. An additional objective was to compare the detection rates of both clinically evident and micrometastatic melanoma in these regional lymph nodes. Twelve pts with histologically confirmed melanoma and clinical evidence of regional node involvement were studied with Tc-99m labeled monoclonal antibody (MoAb) Fab fragment (NR-ML-05 Fab) after a clinical staging evaluation. Planar and SPECT imaging were performed seven hours after the IV injection of 7.5 mg whole (intact) MoAb NR-ML-05 followed by 20 to 30 mCi Tc-99m labeled to 10 mg of NR-ML-05 Fab. Lymphadenectomy was performed the day after imaging. All excised lymph nodes and samples of surrounding normal tissues were weighed and radioactively counted. Thirty lesions were detected by MoAb imaging, 23 were clinically known and 7 clinically unsuspected. Of 19 histologically confirmed melanoma sites, 17 were detected by MoAb imaging (sensitivity, 94%). There was one false positive finding in an area of focal fatty necrosis that was also thought to be positive by physical exam. Of the 12 pts clinically suspected to be Stage II, 8 were found to be Stage II, 3 were correctly downstaged to Stage I, and one pt was correctly upgraded to Stage III based on MoAb imaging and subsequent surgical findings. These results suggest that MoAb imaging may be helpful in the work-up of melanoma patients with suspected lymph node involvement.

Posterboard 1131

TUMOR DIAGNOSIS USING TC-99m MONOCLONAL ANTI-CEA ANTIBODIES

T.Baew-Christow, R.P. Baum, A. Hertel, M. Lorenz, G. Hör. Departments of Nuclear Medicine and Surgery, University Medical Center Frankfurt/Main, FRG.

Over 900 immunoscintigraphic studies have been performed in our department in the last 5 years and established this method as an important diagnostic tool which can decisively influence the clinical management of cancer patients follow up. The successful labelling of Mab with the readily available radionuclide technetium 99m has facilitated the more widespread use of this technique.

The aim of the present study was to evaluate the diagnostic accuracy of a Tc-99m labelled intact anti-CEA Mab (BW 431/26, Behringwerke Marburg) in a prospective protocol. BW 431/26 is of IgG_1 isotype, affinity constant 10^{10} mol/l, direct labelling via Schwarz method. Patients fulfilled the following criteria: increasing serum CEA level strongly indicating potential for tumour recurrence, normal findings in conventional diagnostic procedures (CAT scan, X-ray, ultrasonography, endoscopy).

Out of 180 patients immunoscintigraphy revealed in a prospectively studied subgroup a sensitivity of 73% for occult lesions (sensitivity for known lesions in a retrospective subset was 92%) with a specificity of 88%. Overall diagnostic accuracy was 90% with a positive predictive value of 91% and a negative predictive value of 84%.

Our results demonstrate that immunoscintigraphy with Tc-99m labelled anti-CEA antibody can be routinely performed in an oncological center enabling the earlier diagnosis of tumour recurrences with high diagnostic accuracy which probably will improve the patients prognosis by earlier intervention.

Posterboard 1132

IMMUNOSCINTIGRAPHY (IS) WITH Tc-99m LABELED GRANULOCYTES ANTIBODY (Ab) IN PATIENTS WITH INFLAMMATORY BOWEL DISEASES. A. Kroiss, W. Weiss, Ch. Auinger, T. Feichtenschlager, A. Neumayr. Instit. of Nuclear Medicine, 4th Med. Dep., Ludwig Boltzmann Instit. für klinische Geriatrie, KA Rudolfstiftung, Vienna, Austria.

We wanted to prove the clinical relevance of Tc-99m (BW 250/183; Behringwerke, FRG) labeled Ab in patients with Crohn's disease (C.d.) and ulcerative colitis (u.c.).

We used 20 mCi (740 MBq) Tc-99m and injected the label antibody slowly intravenously. Images were performed 4 hrs and 24 hrs by planar scintigraphy and by SPECT.

With this Ab the imaging was performed in 43 pts, 17 pts with u.c., 26 pts with C.d., 24 female, 19 male, age 35 ± 16 yrs. In these pts we could show the extent of an active bowel disease or demonstrate an inactive bowel disease. We found a sensitivity of 90 % and specificity of 93 % for SPECT imaging.

The results were concordant by the clinical indices, by endoscopy, biopsy, radiography and sometimes surgical specimens. The main advantage of BW 250/183 consists in the fact that the Ab is always available and the labeling procedure with Tc-99m easy to perform.

In conclusion, the method is helpful for localization and extent of active and inactive bowel diseases, there is no in-vitro cell separation necessary and therefore easy to perform. SPECT images are possible.

Posterboard 1133

IMMUNOSCINTIGRAPHY (IS) USING THREE DIFFERENT METHODS OF APPLYING A TC-99m LABELED MONOCLONAL ANTI-CEA ANTIBODY IN STAGING OF PATIENTS WITH LIVER METASTASES BEFORE PARTIAL HEPATECTOMY. N. Rilinger, D.L.Munz, H. Niemann, H.J. Illiger and H.J. Halbfaß. Municipal Hospital of Oldenburg and University of Goettingen, West Germany

It was the aim of this study to determine the value of portal-venous (p.v.), intra-arterial (i.a.) or intravenous (i.v.) IS in the detection of liver metastases before partial hepatectomy in 36 patients (pts) with colorectal carcinoma.

The Tc-99m labeled anti-CEA monoclonal antibody (MAb) BW 431/26 is an IgG1 intact molecule and reacts exclusively with a protein epitope on the CEA complex. Labeling with Tc-99m was described by Schwarz and Steinstraesser (JNM 28: 721, 1987).

Immediately after angiography and i.a. contrast CT (20 pts) or p.v. contrast CT (6 pts), 700-1200 MBq of the Tc-99m MAb were administered via the i.a. catheter. In 10 pts the MAb was injected i.v. Planar scanning with a gamma camera was performed as follows: sequential scanning during the first 5 min, after 10-20 min, 4-6 and 18-30 h p.i., supplemented in special cases by SPECT.

In 25 of the 36 pts metastatic deposits were discovered. IS detected 47/77 liver metastases, 9/10 lymph node metastases and 3/3 local recurrences. In 2 pts IS was the only approach to delineate lymph node metastases.

Despite using 3 different methods (i.a., i.v., p.v.) of applying the Tc-99m MAb in the detection of liver metastases, a total sensitivity of only 61% was obtained. However, IS was still found to be the decisive method of excluding local recurrences and, especially, lymph node metastases before partial hepatectomy.

Posterboard 1134

BIODISTRIBUTION OF I-125-EGF AND ANTI-EGF-R MAB 425 IN TUMORXENOGRAFTS WITH DIFFERENT RECEPTOR DENSITIES. R.Senekowitsch, G.Reidl, R.Niβl and H.W.Pabst. Nuklearmedizinische Klinik, Technische Universität München,FRG

The aim of the study was to assess the epidermal growth factor receptor (EGF-R) status in different tumor xenografts implanted into nude mice in vitro and in vivo with the I-125--receptor ligand EGF and to compare its biodistribution with that of anti-receptor MAb 425 (Merck, Darmstadt). The binding analysis of the EGF-R assay revealed a receptor concentration of 570 fmol/mg protein in breast and and a factor of 10 less in colon carcinoma. The biodistributon data obtained for both substances revealed the rapid biokinetics of EGF in comparison to the MAb, with serum half-lives < 1min for EGF and 2 components for the MAb with 6h and 10d.The whole body half-lives were 2.5h and 6d respectively. The maximum in vivo binding of EGF to the receptor was obtained at 1h p.i. with 3.1% inj. dose/g in breast cancer.A tumor-to-blood ratio of 2 was already obtained at 3-6h p.i., while in colon carcinoma this ratio did never exceed 1. For the MAb the tumor uptake increased until day 9 p.i with values of 20.1 and 6.5% inj. dose/g and tumor-to-blood ratios of 2.4 and only 0.9. The results show the rapid binding of EGF to tumor tissue depending on the receptor density compared to the MAb, offering the opportunity to assess the receptor status in vivo also with short-lifed positron emitters.

Radioassay

Posterboard 1135

RAT MONOCLONAL IMMUNORADIOMETRIC ASSAY SYSTEMS IN MALARIAL ANTIGEN DETECTION. D.K.Hazra, A.K. Gupta,P.K.Wahal,V.K.Suri,S.Yadav,P.K.Bhattacharjee, and A.Saraswat. S.N.Medical College, Agra (U.P.)India.

In view of the limitations observed earlier by us in the Mackey Perrin solid phase RIA for the diagnosis of malarial antigenemia in human subjects, sandwich IRMA systems (conventional reverse and inclusive) based on rat antiplasmodium falciparum monoclonal antibodies were developed. The study material comprised of 10 cases of P.falciparum, 10 of P.vivax and 5 of age and sex matched healthy controls.The same monoclonal was used for coating the solid phase (Dynatech plates) and as labelled antibody in the second layer of the sandwich. The assay was applied to R.B.C.haemolysates and statistically significant higher binding was observed in P.falciparum group as compared to P.vivax and control groups. The subgroups of trophozoites and gametocytes showed almost similar binding. The sensitivity of various systems varied from 80 to 90% while specificity for P.falciparum as compared to P.vivax was 100%. Cases of P.falciparum who were treated showed a fall in the binding signal. There was little correlation between the IRMA binding and degree of microscopic parasitemia.

Posterboard 1136

CATHEPSIN D: A NEW MARKER FOR TUMOR INVASIVENESS. R.Senekowitsch, E.Irmen-Ernst, F.Jänicke, M.Schmitt, A.Hollrieder, H.W.Pabst. Nuklearmedizinische Klinik und Frauenklinik, Technische Universität München,FRG

First clinical results indicate that cathepsin D is secreted in excess by human breast cancer cells and may be correlated with tumor-cell proliferation and invasiveness. The aim of the study was to evaluate a two site radioimmunometric assay (CIS) using 2 monoclonal antibodies against sterically remote antigenic sites on the cathepsin D molecule present in the cytosols of breast cancer tissue. Cytosols were prepared according to the method used for estrogen and progesteron receptors and must be diluted 1/40 and 1/80. In cytosols diluted 1/40 cathepsin values were found 10% higher than after a dilution 1/80. In cytosols thawn and then frozen a second time values approximateley 20 % lower were obtained. Also the buffer used for homogeneization seems to have a considerable influence on the results. In cytosols containing Triton-buffer instead of normal TBS cathepsin values were only 20 %. The coefficient of variation at different concentrations did not exceed 6%. Cathepsin values determined in 104 patients with breast cancer were higher than the cut-off of 60 pmol/mg protein in 33%. The values did not show a correlation to the estrogen and progesteron receptor status but seem to be correlated with tumor invasiveness because most of the metastasis showed clear elevated values.

Hematology/Infectious Disease

Posterboard 1137

SUBTRACTION/REVERSE SUBTRACTION IMAGING (SI/RSI) OF FLORID INFLAMMATORY LESIONS BY COMBINING MONOCLONAL ANTI-GRANULOCYTE ANTIBODY (AGAb) AND NANOCOLLOID (NC): FIRST CLINICAL RESULTS. D.L.Munz, D. Sandrock, A. Enderle, and D. Emrich. Departments of Nuclear Medicine and Orthopedics, Georg August University, Göttingen, Germany.

Scintigraphic localization of inflammatory diseases can present a problem, especially when the foci are located in areas of active hematopoietic or reticuloendothelial bone marrow. Tc-99m labeled AGAb and NC are known to accumulate both in florid inflammatory lesions and in active marrow. Due to the fact that labeled granulocytes are enriched in granulocytic infectious lesions to a higher degree as compared to NC, we applied a subtraction technique to visualize abnormal persisting AGAb uptake surrounded by normally active marrow.

30 patients (18 men, 12 women, aged 49.6 +/- 18.7 years) with suspected infectious lesions (8 in spine, 8 in hips, 9 in lower limbs, 2 in upper limbs, and 3 in other locations) were studied. AGAb scintigraphy (740 MBq Tc-99m anti-NCA 95 AGAb i.v.) was performed as a 4 phase method (flow, early static,2-5 min p.i., and late static images, 4 and 24 hr p.i.) immediately followed by a 3 phase NC scan (370 MBq Tc-99m NC; flow, early static, 2-5 min p.i., and late static images, 30 min p.i.) with the patient in the very same position. Image processing was performed by normalizing the 24 hr AGAb image and the 30 min NC image by using a normal bone marrow region as reference and subtracting NC from AGAb image ("SI") and AGAb from NC ("RSI").

Nine out of 30 lesions had an increased uptake with at least one tracer (5 with AGAb alone, 1 with NC alone, and 3 with both tracers). Subtraction procedure revealed persisting uptake on SI in 5 and on RSI in 2 lesions. Three out of 8 lesions would have been read false positive on the AGAb scan due to accumulation in marrow, which was also seen on NC scan resulting in no persisting activity on SI. In the first 13 cases, SI/RSI was true positive in 4, true negative in 8, and false positive in 1 as confirmed by histology, cytology, bacteriology.

In conclusion, SI/RSI is superior to imaging of inflammatory disease with AGAb or NC alone, especially due to its higher specificity.

Posterboard 1138

IMMUNOSCINTIGRAPHY (IS) USING TC-99m LABELED MONOCLONAL ANTIBODY (MAb) BW 250/183 IN COMPARISON TO RADIOCOLLOID SCANNING IN THE DETECTION OF BONE MARROW (BM) INFILTRATION IN PATIENTS (PTS) WITH SOLID TUMORS AND SYSTEMIC DISORDERS. N. Rilinger 1), M.Z.S. Halabi 1), D.L. Munz 2), H.J. Illiger 1), H. Niemann 1). 1) Municipal Hospital of Oldenburg, 2) University of Goettingen, W. Germany

The aim of this study was to elucidate the value of IS in comparison to radiocolloid scanning in the detection of BM infiltration. We studied a total of 23 pts, 6 with breast cancer, 3 with bronchial cancer, 1 with sarcoma and 13 with Hodgkin (3 recurrences) or Non-Hodgkin lymphoma (stage I-IV). Skeletal scintigraphy, plane radiographs, CT, MRT, and bone marrow biopsies were performed to confirm skeletal/marrow lesions. MAb BW 250/183 is directed against CEA and non-specific cross reacting antigen (NCA) exposed at the cellular membrane of peripheral granulocytes and myelocytes in BM. Labeling procedure with Tc-99m was described by Schwarz and Steinstraesser (JNM 28: 721, 1987). Colloid scanning was done using a commercially available microcolloid kit. 3 h and 1.5 h after injection of 400 MBq Tc-99m MAb and Tc-99m microcolloid, respectively, planar gamma camera scanning of the skeleton was performed.

As compared to microcolloid, MAb showed higher BM uptake with excellent visualization of all bones harboring active BM whereas liver/spleen uptake was moderate. All 40 BM lesions detected by colloid scanning were also seen by IS. However, IS showed 17 additional BM lesions which were all confirmed by the methods mentioned above.

In conclusion, BM IS is superior to radiocolloid BM scanning in the detection of BM lesions in solid tumors and malignant systemic disorders.

Pediatrics

Posterboard 1139

USING THE RADIONUCLIDE SALIVAGRAM TO DETECT PULMONARY ASPIRATION AND ESOPHAGEAL DYSMOTILITY, K.Levin, A.Colon, J.DiPalma, S. Fitzpatrick, Georgetown University Hospital, Washington, DC.

Our experience with the radionuclide salivagram (1) and its ability to detect aspiration in children is reviewed in this study. The radionuclide "milk" scan is insensitive for aspiration. 0.5-1.0 mCi Tc-99m Sulfur Colloid in less than 1cc is instilled into the mouth, and supine posterior images of the thorax are obtained for an hour with delayed images until the oropharynx is clear.

Studies (14) were performed in 13 patients ages 1 month to 6.5 years suspected of aspirating. The scintigraphic findings demonstrate aspiration in 4 of 14 (28%); dysmotility (prolonged esophageal activity) in 7 of 14 (50%); and normal in 3 of 14 studies (22%). Of 13 patients, 8 had milk scans negative for aspiration. One patient studied twice had aspiration on the first study and dysmotility on the second.

We conclude that the salivagram can detect aspiration of oral secretions, is superior to the milk scan in detecting aspiration, and can demonstrate esophageal dysmotility.

(1) Heyman, S, Respondek, M, Detection of Pulmonary Aspiration in Children by Radionuclide "Salivagram"., J Nucl Med 30:697-699, 1989.

Renal/Electrolyte/Hypertension

Posterboard 1140

MEASUREMENT OF THE GLOMERULAR FILTRATION RATE WITH AN AMBULATORY RENAL MONITOR. M. Juweid, R.H. Moore, A.J. Fischman, H.W. Strauss, C.A. Rabito. Massachusetts General Hospital, Boston, MA.

It is well known that the plasma level of creatinine [CR] is not a good indicator of the renal function especially in patients with severe renal disease. More accurate measurements of the renal function such as GFR require the use of clearance technique, usually more difficult to perform.

We describe a simple method to indirectly measure the GFR using an arm-worn ambulatory renal monitor. A scintillation detector placed in a lead-lined blood pressure cuff, attached to a miniaturized multiscaler, was employed to monitor the clearance of 99mTc-DTPA activity from tissue background as an indicator of the GFR. The miniature NaI detector system records activity directly to memory at user-programmable intervals. Data can be directly analyzed or transferred to a PC for plotting and archiving.

The measurements were started after a routine renal scintigraphic study usually 60-90 minutes after injection. Using a one compartment model, the rate constants in 3 subjects with creatinine values within normal range were 7.8, 7.9, 4.5 x 10^{-3} min^{-1}, while in three subjects with creatinine values of 1.8, 2.3, 3.8 mg/dl, respectivly the rate constants were 3.2, 3.15, 1.8 x 10^{-3} min^{-1}, respectively.

These results suggest that the renal function can be readily monitored by clearance of DTPA using an ambulatory device.

Posterboard 1141

EFFECT OF SHORT TRANSIT TIMES ON GFR ESTIMATION FOR RENAL TRANSPLANTS. K.C. Young and I. Hassan. Dept. of Nuclear Medicine, Faculty of Medicine, Kuwait.

Gates' method of estimating GFR relies on renal uptake at 2-3 minutes and on the assumption that the minimum transit time (minTT) is more than 3 minutes. We have applied the method to renal transplants by estimating the kidney depth from lateral views. The calculated GFR was lower than expected in some patients, and this study investigated whether this was due to rapid renal transit.

Thirty-six patients were studied; 24 had baseline Tc-99m DTPA renograms within 24 hours of receiving renal grafts from living related donors and 12 donors had renogram studies prior to surgery. From the renogram data the GFR was estimated for each kidney using Gates' method and a modification using a 1-2 minute uptake. The minTT was determined for each kidney as the time when activity first appeared in the ureter or bladder.

Thirty-seven kidneys with minTT in excess of 3 minutes had uptakes at 2-3 and 1-2 minutes which were linearly correlated (r=.96±.01) with a mean ratio of 1.11±.01 (s.e.m). Using this data comparable GFR values were estimated using either uptake.

Fourteen of the transplanted kidneys had minTT of less than 3 minutes and in 6 of these the minTT was less than 2 minutes. In these patients the standard Gates' method resulted in estimates of GFR which were up to 40% less than when using the 1-2 minute uptake.

Gates' method cannot be reliably applied to transplanted kidneys as transit times of much less than 3 minutes may occur. Modifying the method to use 1-2 minute uptake resulted in more reliable estimates of GFR

Posterboard 1142

TECHNETIUM-99m HMPAO LABELED WBC'S IN THE DETECTION OF ACUTE APPENDICITIS. D.S. Rimkus, C. Foley, and R. Lattimer. Cottage Hospital, Santa Barbara, CA.

Nine patients (5 female, 4 male) with suspected acute appendicitis were imaged with Tc-99m HMPAO labeled WBC scans in a blinded study. Images were obtained immediately (under 30 minutes), and 1.5 to 3 hr after reinjection of 5 mCi Tc-99m HMPAO labeled WBC's. Surgically excised appendices were also imaged.

Seven patients had appendectomes. Five of these patients had acute appendicitis; two were negative. In the 5 positive patients, 4 had positive scans within 30 minutes. The fifth patient's immediate scan was negative; delayed images could not be obtained because of immediate surgery, but the removed appendix was positive at imaging. Two surgically proven negatives, and two clinically negative patients had negative scans. There were no false negative scans at 1.5 to 3 hr.

This data yields a sensitivity of 80% for immediate images, 100% for delayed images, and a specificity of 100%.

Tc-99m HMPAO labeled WBC's offer a rapid, readily available test for acute appendicitis.

Instrumentation & Data Analysis: General

Posterboard 1143

CAUTION IN THE USE OF THE 167-KEV PEAK FOR TL-201 IMAGING. M.V. Yester. The University of Alabama at Birmingham, Birmingham, AL.

For Tl-201 imaging a 15 - 20% window centered on the Hg x-rays is used typically. It is also common to use a 20% window centered on the 167-keV gamma ray. Due to contamination of Tl-200 and Tl-202, there is spill down from the higher energy gamma rays of these nuclides. In order to study the affect of this, spectra were obtained from a scintillation camera by intercepting the energy signal from the camera and routing it to a computer-based multichannel analyzer. Spectra were obtained for the source in air without a collimator, in air with a general purpose collimator, and in an Adam's phantom (for scatter simulation) also with the general purpose collimator. Using a 15% window for the Hg x-rays and a 20% window for the 167-keV peak, total counts were calculated. There was a net gain in count rate for the 167-keV peak in scatter medium relative to the Hg x-rays. The actual measured 167-keV/Hg x-ray ratio was 13%. The difficulty is that the background from the high energy gamma rays in the 167-keV window was 30% of the total counts in the window. Thus 30% of the 13% increase from using the 167-keV peak is due to scattered photons. This contamination is dependent on the lot number and on the age of the thallium, i.e. for Tl-201 close to the expiration date, the background ratio will be even higher. In addition the second peak could produce a further loss of resolution due to multiple energy registration effects. Thus, it would seem that the gain in use of the 167-keV peak is marginal.

Posterboard 1144

EVALUATION OF CRT DISPLAY PARAMETERS USED IN CLINICAL INTERPRETATION OF DIGITAL NUCLEAR MEDICINE IMAGES. D.J. Wagenaar, A.M. Cohen, R. Nawfel, and P.F. Judy. Joint Program in Nuclear Medicine, Harvard Medical School, Boston, MA.

In order to optimize the presentation of digital scintigrams to physicians, we have studied physician visual preferences in the Division of Nuclear Medicine at Boston's Beth Israel Hospital. The digital-to-analog conversion process and the function of the intensity and contrast controls are reviewed. Each of three attending physicians used the same CRT, a Panasonic WV-4590, to read ten separate studies for each of four nuclear medicine procedures. For each reading the physician adjusted the intensity and contrast settings to his personal preference, as well as the window for digital image display. Following each reading the luminance (in fL) versus input value (0-255) was measured with a photometer and the SMPTE test pattern. The histogram of input values for each reading was plotted and the window settings for each reading were recorded. In nearly all of the readings the monitor was adjusted such that a 5% difference in the input at both the light and dark extremes could be perceived. Parameters such as peak pixel count luminance and average pixel luminance were derived from the histogram and luminance data. Correlations were made by analyzing these parameters in terms of both individual physicians and study types. Although the luminance curves varied between physicians, for a given physician consistent preferences were found for each study type. Protocols for obtaining monitor settings using the SMPTE pattern are suggested.

Work supported by NIH Grant #1 RO1-CA43114.

Posterboard 1145

AN IMPROVED IMAGING DETECTOR FOR CHARGED PARTICLE EMITTING RADIONUCLIDES. K. Ljunggren, S.E. Strand. Department of Radiation Physics, University of Lund, Sweden.

We previously reported on the development of a new detector system that is capable of static and dynamic imaging of charged particles emitted by radionuclides distributed in tissue slices. The new detection system consisting of a plastic scintillator and an improved light sensitive detector is reported here. The light photon sensitive detector consists of a fiber-optic window, a photo-cathode, three microchannel plates and a resistive anode. The resistive anode is connected from each corner to four amplifiers coupled to an ADC.

A new image memory and an acquisition unit (IMU) is constructed in our laboratory based on the Motorola 68000 microprocessor and the VME bus. The IMU provides unique opportunities to normalize and discriminate without changing the raw data. The IMU is connected to the host 80386-computer via a 2x8 bits parallel interface. The ability to image the beta-particles emitted by 90-Y labeled antibodies was tested. Nude mice bearing xenografted human serous ovarian cancer were injected with 90-Y labeled monoclonal antibodies reacting against fibrin (59D8 Fab fragment, provided by Dr. Kairemo, Helsinki). Tumor tissue was taken out and prepared for imaging on the beta camera. Images of high quality were acquired within minutes. We have improved our imaging detector which is capable of detecting charged particle emitting radionuclides distributed in biological samples. With this system it is possible to make very rapid acquisitions compared to conventional filmautoradiographic-technique, as well as to perform dynamic studies on living samples.

Posterboard 1146

LOCALIZATION OF INFLAMMATORY BONE LESIONS BY DOUBLE TRACER SUBTRACTION/REVERSE SUBTRACTION IMAGING - PHYSICAL AND PHYSIOLOGICAL CONSIDERATIONS OF A NEW APPROACH. D. Sandrock and D.L. Munz, Department of Nuclear Medicine, Georg August University, Göttingen, Germany.

Objectives of this study were to develop an optimized double tracer subtraction technique based on physical and physiological considerations for the localization and differentiation of inflammatory bone lesions. The rationale of the new procedure was to use a monoclonal anti-granulocyte antibody (AGAb), which accumulates in florid granulocyte infections but also cross-reacts with normal bone marrow, and nanocolloid (NC) as a bone marrow tracer to overcome this cross-reactivity by subtraction.

Phantom studies (water phantom with Tc-99m sources of various activities simulating inflammatory lesions/background/ bone marrow/blood vessels) revealed a minimal count rate of 1000 net counts (= remaining counts after subtraction) per lesion for reliable count statistics. In order to obtain these counts rates in patients, minimal activities of 740 MBq for AGAb and 370 MBq for NC are required.

In all patients, dynamic flow studies, early (2 min p.i.) and late (4, 24 hr p.i.) static images were obtained following i.v. injection of 740 MBq Tc-99m monoclonal anti-NCA 95 AGAb. After the 24 hr image, 370 MBq Tc-99m NC were injected without moving the patient and dynamic flow study as well as early (2 min p.i.) and late (30 min p.i.) static images were obtained.

Subtraction procedure was performed with the 24 hr AGAb image and the 30 min NC image. Normalization of both images was done by using a region of interest over normal bone marrow and calculating a multiplication factor for each image in order to get equal count rates in the reference region. The normalized NC image was then subtracted from the normalized AGAb image. Persisiting activity on the subtraction image was read "positive" for a florid granulocytic infection. For the "reverse subtraction", normalization was done the same way, but AGAb image was subtracted from NC image. Persisting activity on the "reverse subtraction" image was interpreted as sign of a local macrophage process or specific inflammation.

Up to now, the protocol has been tried in 25 patients with encouraging results (92 % accuracy in the first 13 patients with follow-up). Thus, it seems to be a promising technique which overcomes the problem of bone marrow cross-reaction of anti-NCA AGAb for the localization of inflammatory bone lesions.

Posterboard 1147

MATHEMATICAL MODELING OF ANTIBODY DISTRIBUTION IN MAN. A. Rescigno, H. Bushe, A.B. Brill. University of Massachusetts Medical Center, Worcester, MA.

Many papers on the pharmacokinetics of labeled monoclonal antibody (Ab) limit their scope to analysis of plasma clearance curves. From these analyses, clearance half-times and volumes of distribution are computed. Previous investigators have analyzed Ab blood clearance curves as if only a single species was present, whereas two or more distinct chemical forms frequently are present. As a result, clearance half-times and volumes of distribution are inherently in error. We used analytical techniques to measure the number and concentration of radiolabeled species in patient sera. These measurements, along with the amounts of label in normal organs and in tumor, were used to model the radiolabeled C110 Ab kinetics in patients.

We used the method of Beck and Rescigno (J. Theoret. Biol. 6:1-12, 1964) to determine the precursor-product relationships between different organs, and non-compartmental methods to compute transit time, permanence time, residence time, and yield. The results indicated that blood antibody complexes formed in serum are extracted by liver, and breakdown products are extracted in urine.

Instrumentation & Data Analysis: PET

Posterboard 1148

INVESTIGATION OF COMPARTMENTAL MODELS FOR ESTIMATION OF L-[2-^{18}F]FLUOROTYROSINE TRANSPORT AND PROTEIN INCORPORATION RATE IN ISOLATED RAT HEART. T.R. DeGrado, H.H. Coenen, G. Stöcklin. Institut für Chemie 1, Forschungszentrum Jülich, FRG

Compartmental model structures relevant for quantitative estimation of tyrosine transport and protein incorporation rates (PIR) using L-[2-^{18}F]fluorotyrosine (L-2FTyr) were investigated in Langendorff perfused rat hearts with external γ,γ-coincidence detection. Inhibition of protein synthesis by anoxia or 0.02 mM cycloheximide provided a four-fold range of PIR over which the modeling technique could be evaluated. HPLC analysis of tissue homogenates showed > 98% of the label to be as L-2FTyr or protein-bound throughout a 1 hr period. A three compartment model including vascular L-2FTyr, tissue L-2FTyr, and irreversibly bound protein compartments could fit the initial uptake and early clearance rate but failed to describe the slower clearance rate following 20 min of washout. Model predicted values of labeled protein fraction and PIR were consistently overestimated. The overestimation increased as PIR decreased. With the addition of a second tissue L-2FTyr compartment in communication only with the first, the entire residue curve was adequately fit but PIR remained slightly overestimated. Transport was well described by both models, showing no diminution with anoxia or cycloheximide. By contrast, the myocardial kinetics of the D-stereoisomer of 2FTyr, which was poorly transported and not incorporated into protein, could be adequately modeled with a single tissue compartment.

Posterboard 1149

QUANTITATIVE PERFORMANCE ANALYSIS OF 3D INTERPOLATION ALGORITHMS FOR REORIENTATION OF CARDIAC PET IMAGES. W. Kuhle, G. Porenta, M. Phelps, H. Schelbert. UCLA School of Medicine, Los Angeles, CA.

The transaxial orientation of cardiac PET images causes considerable inter- and intrapatient variability of regional activity concentrations. Image reorientation into standard short-axis cross sections of the heart minimizes the variability of image data and is accomplished by 3D interpolation. However, interpolative algorithms distort the original data. Quantification of physiologic processes from the reoriented images therefore requires characterization of errors introduced by interpolation. Determinants of errors include the type of interpolation algorithm, the angle through which the original images are rotated and the ratio of the axial plane spacing to the in-plane pixel size. An annular cardiac phantom was imaged in a 15-plane CTI 931 tomograph at six angles (0°, 5°, 25°, 45°, 65°, 85°) in the tomograph's azimuthal plane and at two different bed positions for each angle. The two bed positions allowed for interleaving of planes, thus doubling the axial sampling and halving the plane spacing to pixel size ratio. A 0.30 Shepp-Logan filter was used to reconstruct and two different interpolators were used to reorient the images. One used standard 3D linear interpolation (LI) and the other used a novel hybrid interpolation (HI), consisting of LI in-plane and cubic convolution across planes. Circumferential profile analysis of the reoriented phantom images revealed a maximal loss of counts at 65° for both interpolators, with LI losing 10% ($p<.0001$) and 6.5% ($p<.0001$) and HI losing 6% ($p<.0001$) and 5% ($p<.0001$) in the non-interleaved and interleaved cases, respectively. Count loss varied with angle, but HI lost fewer counts than LI at all angles ($p<.0012$). Thus, reorientation of cardiac images into short axis views introduces error into quantitative image analysis and requires characterization of the effects of axial sampling, reorientation algorithm and reorientation angle on the error. While reorientation causes a loss of counts, the loss can be minimized by a new 3D hybrid interpolation algorithm.

Instrumentation & Data Analysis: SPECT

Posterboard 1150

CARDIAC SPECT IMAGING WITH FAN BEAM COLLIMATORS. G.T. Gullberg, P.E. Christian, F.L. Datz, G.L. Zeng, C. Yu, X. Wang, B.M.W. Tsui, J.R. Perry, H.T. Morgan. The University of Utah, Salt Lake City, UT; The University of North Carolina, Chapel Hill, NC; and Picker International, Highland Heights, OH.

Fan beam collimators have been developed to increase the detection efficiency in cardiac SPECT imaging by taking advantage of the large field of view rotating gamma camera used in current SPECT systems. Studies with two fan beam collimators (one with 60 cm focal length, 8 mm FWHM at 10 cm; the other with 70 cm focal length, 10 mm FWHM at 10 cm) have been conducted on phantoms and patients. A critical factor in our studies was focal length requirements. Magnification limits were closely studied so that the heart remains in the field of view. The 60 cm focal length collimator was designed to improve detection efficiency and maintain the same resolution as the general purpose parallel hole collimator. Since the fan beam collimator magnifies the data causing the distribution in tissue surrounding the heart to extend outside the field of view, algorithms had to be developed to correct for data truncation. Several truncation algorithms have been investigated and in general, most work well in eliminating reconstructed ring artifacts due to the fact that data truncation usually occurs only in the low background tissue activity. The truncated, corrected fan beam data are reconstructed using a new reconstruction algorithm that reconstructs fan beam data obtained from a noncircular orbit scanned over 180° around the patient. Clinical results indicate improved lesion observability compared to results obtained with the general purpose parallel hole collimator (8.2 mm FWHM at 10 cm).

Posterboard 1151

CLINICAL INVESTIGATION OF MAXIMUM VALUE REPROJECTION FOR SPECT IMAGING. F.D. Thomas and S.H. Manglos, University Hospital, SUNY Health Science Center at Syracuse, Syracuse, NY, and R.W. Walker, Trionix, Twinsburg, OH.

The number of images produced in a typical SPECT study can be fatiguing and time consuming to analyze and cross correlate. Reprojection is a technique which allows substantial condensation of this volume while producing a 3 dimensional representation. Starting with a standard filtered and back projected reconstruction, this technique reprojects data back into a set of 2 dimensional matrices using all of the events along each ray. If simply summed, this results in an image analogous to a high count density planar acquisition but the contrast produced from a SPECT reconstruction is lost.

We have investigated a clinically more useful reprojection method ("maximum value"), which uses the pixel with the highest value along each reprojected ray. The inherent contrast is retained and local anatomic detail is rendered in high dimensional clarity. A distance weight is applied during reprojection to provide the illusion of depth which also allows the observer to determine the direction of rotation, and thus body right vs left, in a rotating cine display. This technique differs fundamentally from the conventional 3-D surface display which uses an edge threshold, suited to objects with single surface features.

After clinical trials with many patients, we have found maximum value reprojection to be an important, sometimes critical, clinical tool in SPECT studies of bone disease, lymphomas, hemangiomas, gated ventriculograms and myocardial infarct imaging. Although this technique does not eliminate the need for slice data, it allows a quicker review of the entire volume and provides diagnostically useful supplemental viewing.

Posterboard 1152

DETERMINATION OF INFARCT SIZE BY A NEW QUANTITATIVE ANALYSIS OF CARDIAC PERFUSION TOMOGRAPHY. L. Mortelmans, J. Nuyts, P. Suetens, F. Van de Werf, A. Oosterlinck, M. De Roo. U.Z. Gasthuisberg, K.U.Leuven, Leuven, Belgium.

The study was performed to compare the perfusion defect (P.D. tomo) delineated by a new quantitative

analysis (J Nucl Med; 30 : 1992-2001, 1989) to enzymatic infarct size (Enz. I.S.), global left ventricular function (LVEF) and perfusion defects on planar scans (P.D. planar).

49 patients pertaining to a double-blind rt-PA vs placebo study and 60 patients treated with rt-PA were referred 10 to 14 days after AMI. They underwent a SPECT study after injection of 2 mCi Tl-201 and 20 mCi MIBI respectively. P.D. was determined using 1, 2 or 3 s.d. as cut-off level on the polar maps. Enz. I.S. was determined by serial determination of α-hydroxybutyrate dehydrogenase (HBDH Q72) and LVEF was measured by contrast angiography (Angio). The P.D. on planar images was determined by a circumferential profile method.

The relationship between tomographic P.D. and the other parameters is expressed by a Spearman correlation coefficient (cfr. table). The delineation of the ventricular wall, the apex and the valve plane was satisfactory especially for the MIBI studies.

	Enz. I.S.	LVEF (angio)	P.D. (planar)
P.D. (Tl-201)	0.52-0.54	-0.70; -0.65	0.67-0.68
	0.75-0.76	-0.68; -0.63	0.81-0.88

It can be concluded that the good correlation with Enz. I.S. and LVEF proves the validity of our new delineation algorithm for automatic determination of P.D. on thallium and MIBI tomographic studies.

Posterboard 1153

INAPPROPRIATE MOTION CORRECTION DUE TO BREAST ATTENUATION IN THALLIUM SPECT. HR Balon, JE Juni and RA Ponto. William Beaumont Hospital, Royal Oak, MI.

Patient motion during Tl-201 SPECT acquisition may produce image artifacts. Software for motion correction by detection of vertical pixel shift between consecutive projections is now commercially available (General Electric). We postulate that attenuating tissue extrinsic to the heart (in particular, breast) may cause the GE algorithm to falsely detect vertical motion and inappropriately shift projection images. We suggest that a surface point marker would provide a dominant reference signal for the algorithm and reduce this error.

A 500 ml plastic IV bag of saline was attached to a chest/heart phantom, partially overlapping the heart, to simulate attenuation from breast tissue. Four Tl-201 SPECT acquisitions were performed with and without the breast attenuator, with and without a prominent Tl-201 point source placed inferior to the heart apex, and with and without motion. The GE motion correction program was applied to all data. In the absence of motion, the presence of the breast attenuator caused the program to inappropriately detect motion of 1.76 pixel± .24 (1 SD) (1 pixel=6mm). The image shift was reduced to 0.69± .32 pixel using the point source ($p < 0.0008$). This residual shift was comparable to the "noise" of acquisition of the phantom alone (.53± .18 pixel)($p=.35$;NS). Effects of the breast attenuator were similar when a 2 pixel cephalad motion was introduced during acquisition: a 4.0± .09 pixel shift was detected which was reduced to 2.65± .4 pixels with the point marker ($p < 0.008$).

Although it may compromise the ability to correct for "cardiac creep", we suggest that an external point source be used in female pts with substantial breast tissue.

Dosimetry/Radiobiology

Posterboard 1154

RADIATION DOSIMETRY FOR PHOTON SOURCES DISTRIBUTED OVER THE SURFACE OF THE HUMAN EYE. M. Stabin, Oak Ridge Associated Universities, Oak Ridge, TN, A. Hawi, G.A. Digenis, University of Kentucky, Lexington, KY.

Gamma scintigraphy is a simple, non-invasive, and precise technique for assessing the in-vivo behavior of certain ophthalmic preparations labeled with radiotracers. The techniques needed to assess the radiation dosimetry for this application are not addressed in the published MIRD or ICRP literature. We therefore constructed a model of the eye for the purposes of modeling radiation transport, and estimated the spatial distribution of dose within the model given a source covering the (model defined) exterior surface of the eye. We employed the energy deposition formulas of Spencer and Simmons (Nucl Sci and Eng, 50:20-31, 1973) and the photon mass attenuation coefficients for soft tissue of Hubbell (Int J Appl Rad Isot 33:1269-1290, 1982). We generated S-values as a function of position in the eye and isodose contours (based on measured residence times) for Cr-51, Tc-99m, In-111, Ce-141, Sm-153, and Er-171, tracers we are considering for labeling of the ophthalmic preparations. We also considered the radiation dosimetry of the GI tract from drainage of the tracers through the nasolacrimal apparatus.

Work supported partly by contract No. DE-AC05-76-OR00033 with the Department of Energy and Interagency Agreement FDA 224-75-3016 with the Food and Drug Administration.

Posterboard 1155

RADIOPHARMACOLOGY AND TISSUE LOCALIZATION OF INDIUM-111 SUBSTANCES EVALUATED IN THE RAT APRROACHING AUGER ELECTRON DOSIMETRY.
B.A. Joensson and S.E. Strand. Department of Radiation Physics, University of Lund, S-221 85 Lund, Sweden.

It was early recognized that Indium-111 and the accompanying impurity In-114m give high absorbed doses to the patient after administration of a radiopharmaceutical. It has also been demonstrated that In-111 is extremely radiotoxic when localized within or close to the cell nucleus, due to emitted conversion and Auger electrons during the decay. In conventional internal dosimetry it is assumed that the radionuclide is homogenously distributed in the whole volume of an organ and therefore the absorbed dose to individual cells in the tissue is the same as the mean absorbed dose to the entire organ. Thus the knowledge of the localization of the radionuclide is essential in order to perform reliable absorbed dose calculations and to determine the radiation hazards.

This study was undertaken to achieve more and necessary information about the biokinetics of In-111 labeled biomolecules, and to investigate the activity distribution and activity concentration in different tissues and part of tissues. Different In-111 radiopharmaceuticals were injected into rats, which were followed up to 1 month. Activity in blood, plasma, urine, faeces and most tissues was measured at different time points. Digital quantitative whole body autoradiography was executed to investigate the activity concentrations in some important tissues.

Our results show highest activity uptake in rapid proliferating tissues (bone marrow, lymph nodes, testes and spleen) i.e. those tissues characterized as very radiosensitive. In addition, the radionuclide is retained for a long period of time. Also liver and kidney have a considerable accumulation of indium. The autoradiography shows that in many tissues e.g. spleen, liver, bone marrow, testes and kidney, the radionuclide is very inhomogenously distributed.

Our research demonstrate the importance of careful investigations of the pharmacokinetics including exploration of the activity distribution within tissues evaluated by quantitative autoradiography. The study confirm the need for an improved internal dosimetry and show the limitations of the current conventional MIRD-dosimetry which may underestimate the absorbed dose because of unknown localization data.

Nuclear Magnetic Resonance

Posterboard 1156

REPORT OF ONGOING CLINICAL TRIALS OF Gd(HP-DO3A), A LOW OSMOLAL MR CONTRAST MEDIUM. M. Carvlin, L. Rosa, D. Schellinger, J. Francisco. Goergetown University Hospital, Departments of Radiology and Neurosurgery, Washington, DC.

At present there is a single contrast agent, gadopentetate dimeglumine (Schering/Berlex), that has received FDA approval for use in MRI. This material is administered as the 0.5 M solution at a dosage of 0.1 mmol/kg and has an osmolality of 1940 mOsmol/kg. In comparison, the agent under test is a lower osmolar solution (630 mOsmol/kg) of the neutral gadolinium chelate, Gd(HP-DO3A) (Squibb Diag), in which the chelator is 1,4,7-tris(carboxymethyl)-10-(2'-hydroxypropyl)-1,4,7,10-tetraazacyclododecane. We have evaluated the efficacy and safety of Gd(HP-DO3A) in 32 patients with symptoms of intracranial disease (n=20) and spinal disease (n=12). Gd(HP-DO3A) was administered intravenously at dosages of 0.05 (n=1), 0.1 (n=29), 0.2 (n=1), 0.3 (n=1) mmol/kg. Short TR/TE (pre- and post-injection) and long TR/TE (pre-injection) spin echo images were obtained using a 1.5 Tesla (Siemens) MRI. Physical examination, vital signs, hematology, urinalysis and biochemical blood tests were performed within 24 hrs preceding and following administration of the agent. Signal enhancement of areas of abnormal capillary permeability associated with intracranial and spinal diseases were conspicuous findings in post-contrast images. Tumor boundaries, meningeal involvement, abnormal vascularity, herniated disc, epidural scar were judged to be better distinguished in post-contrast images. Gd(HP-DO3A) was uniformaly well tolerated with no significant adverse reactions and no significant abnormalities in the laboratory tests that were felt to be drug related. Insofar as Gd(HP-DO3A) has lower osmolality and greater kinetic inertia to Gd(III) dissociation,higher dosages and new applications may be examined.

Radiopharmaceutical Chemistry: Proteins/Antibodies

Posterboard 1157

PREPARATION AND CHARACTERIZATION OF RADIOACTIVE POLYCHELATES AND THEIR ANTIBODY CONJUGATES.
P. F. Sieving, A. D. Watson, and S. M. Rocklage.
Salutar, Inc. Sunnyvale, CA

There have been numerous attempts, with varying degrees of success, to attach chelates to antibodies and proteins in order to site-specifically deliver metal ions in vivo for diagnostic and therapeutic applications. Chelates with high thermodynamic and kinetic stability characteristics are mandatory, to avoid metal ion release with concommitant toxicity and dosimetry problems; the tetraazatetracarboxylate macrocycle DOTA is an appropriate choice. Poly-L-lysine (PL, degree of polymerization 100) was N-acylated with the mono-mixed anhydride of DOTA, to provide a non-crosslinked polychelate containing 60-90 chelating groups per molecule. This was purified by size-exclusion chromatography and conjugated to HSA with standard heterobifunctional cross-linking reagents to provide a potential blood-pool diagnostic agent. Biodistribution data has been obtained using Gd-153-labelled conjugates. Separately, conjugation of the polychelate to both L6 and CAT-301 monoclonal antibodies has been accomplished, and the incorporation of Y-90, In-111 and Sm-153 is envisaged. MRI studies with these systems, following incorporation of Gd and Dy, will also be described.

Radiopharmaceutical Chemistry: Positrons

Posterboard 1158

"NO CARRIER ADDED" C-11 LABELLING OF THE ALKYLATING CHEMOTHERAPEUTIC AGENT BUSULPHAN. M. Hassan, J.O. Thorell, S.A. Stone-Elander, H. Ehrsson, L. Widén and K. Ericson. Karolinska Pharmacy and Depts of Clinical Neurophysiology & Neuroradiology, Karolinska Institute, Stockholm, Sweden

Busulphan is an antileukemic agent, mainly used for the treatment of chronic myelocytic leukemia. In the past few years a great interest has been focused on the drug in connection with bone marrow transplantation. Recent studies in the rat have shown that busulphan is transported across the BBB. Human studies have also shown a rapid distribution of busulphan into the CSF. Reports of epileptic convulsions in connection with high-dose treatment have raised questions about central nervous system toxicity. Carbon-11 labelling of busulphan would enable in vivo PET studies of its biodistribution.

The radiolabelling consists of five steps including purification. Aqueous C-11-cyanide was reacted with 3-bromo-1-propanol (7 min, 90 C) followed by an acidic hydrolysis (10 min, 140 C) to form gamma-hydroxybutyric acid lactone. After elution through Sep-paks, the lactone was reduced to 1,4-butanediol using lithium aluminium hydride. The diol was reacted with methanesulfonic acid anhydride (3 min, 20 C) to form [1-11C]-1,4-bis(methanesulfoxy)butane (busulphan). The product, isolated by reversed-phase HPLC, was shown to be >99% radiochemically pure. After filtration through a Millipore filter, a sterile solution free from pyrogens (Limulus test) was available for PET studies of its in vivo distribution in animals or humans. Total time of synthesis was 60-70 min from E.O.B. and total radiochemical yield was approximately 10-20%, based on trapped cyanide.

Posterboard 1159

AN IMPROVED ANION EXCHANGE RESIN COLUMN FOR DIRECT NUCLEOPHILIC F-18 RADIO FLUORINATION. D.M. Jewett, S.A. Toorongian, and W.M. Walker. Division of Nuclear Medicine, University of Michigan Medical School, Ann Arbor, MI 48109-0552.

Problems with column plugging or excessive back pressures resulting from resin particle aggregation were significantly reduced when the resin particles were interspersed during packing with inert, nonporous particles (sulfonated polyethylene, H^+ form) of opposite charge. For [F-18]FDG 17 mg of the Merrifield resin (4-methyl-4-piperidinopyridine, carbonate form) was suspended with 8.5 mg of polyethylene particles in 1 ml 30% aqueous ethanol, and slurry packed in a 1.3 mm I.D. Teflon column. The column was washed with pure water and dried for 10 min by a flow of N_2. In a typical radiolabeling reaction, 1 ml [O-18]water from a silver target was passed through the column, which trapped 360 mCi (94%) of [F-18]fluoride. The column was dried with 2 ml MeCN at 24°, and 1 ml more MeCN while the temperature was raised to 95°. Then 25 mg of mannose triflate in 2 ml MeCN were passed through the column at 95° followed by 1 ml MeCN to elute 85% of the radioactivity. The uncorrected yield of [F-18]FDG after evaporation of the MeCN and acid hydrolysis was 51%. The resin was prepared by chlorosufonylation of UHMW polyethylene powder with SO_2Cl_2 in CCl_4/pyridine in the presence of AIBN, followed by hydrolysis.

Posterboard 1160

Synthesis of No-Carrier-Added ^{18}F-and ^{11}C-Labeled Methamphetamine and its Analogs. C.-Y. Shiue, G.G. Shiue, R.B. Sharma and M.P. Frick. Creighton University, Omaha, NE.

Methamphetamine and 3,4-methylenedioxymethamphetamine ("Ecstasy") are the widening used illicit drugs. In order to characterize their in vivo binding properties with PET, we have synthesized [^{18}F]methamphetamine (1b) and its analogs. Compound 1b was synthesized from p-nitrobenzaldehyde with ^{18}F ($K^{18}F$/kryptofix, DMSO, 140°C, 10 min), followed by Knoevenagel condensation with nitroethane (110°C, 10 min.), reduction with $LiAlH_4$ and methylation with CH_3I to give 1b in ~7% yield in a synthesis time of 100 min. from EOB. Attempt to synthesize 2b from 2a resulted in a low yield. ^{18}F-labeled "Ecstasy" (1d) was synthesized from 6-nitropiperonal in a similar manner in an overall yield of ~5% in a synthesis time of ~100 min. from EOB. Methylation of amphetamine and 3,4-methylenedioxyamphetamine with CH_3I (DMSO-DMF, CH_3CN, 150°C, 5 min.) gave methamphetamine and Ecstasy in high yield. The synthesis of ^{11}C-labeled methamphetamine, Ecstasy and the studies of their in vivo binding properties are currently under investigation.

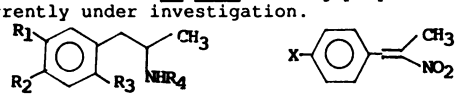

1a) $R_1 = R_3 = R_4 = H$, $R_2 = {}^{18}F$
1b) $R_1 = R_3 = H$; $R_2 = {}^{18}F$, $R_4 = CH_3$
1c) $R_1, R_2 = OCH_2O$; $R_3 = {}^{18}F$; $R_4 = H$
1d) $R_1, R_2 = OCH_2O$; $R_3 = {}^{18}F$; $R_4 = CH_3$

2a) $x = NO_2$
2b) $x = {}^{18}F$

Posterboard 1161

POSITRON-LABELED MONOAMINE OXIDASE (MAO) INHIBITORS: SYNTHESIS OF [F-18]FLUOROPARGYLINE AND N-(4-[F-18]-FLUOROBENZYL)PROPARGYLAMINE.
D.-R. Hwang, J.L. Gong, M.J. Welch. Mallinckrodt Institute of Radiology, Washington University School of Medicine, St. Louis, MO.

Pargyline, N-benzyl-N-methyl-propargylamine, is a potent MAO inhibitor. Recently, its demethylated metabolite has been shown to be a specific MAO-B inhibitor. To evaluate the possibility of using [F-18]-labeled MAO inhibitors in probing MAO activity in vivo by PET, we prepared [F-18]fluoropargyline, (1), and N-(4-[F-18]-fluorobenzyl)-propargylamine, (2). Compound (1) was prepared via a one-pot two-step procedure: a F-18-for-nitro exchange reaction with 4-nitrobenzaldehyde followed by a reductive amination reaction using N-methyl-propargylamine and sodium cyanoborohydride, with a radiochemical yield of 15% and a specific activity >500 Ci/mmol in a synthesis time of 1 h. Same one-pot procedure failed to yield compound (2). When [F-18]-fluorobenzaldehyde was purified before the reductive amination reaction with propargylamine, compound (2)

was prepared with a radiochemical yield of 10% and a specific activity of > 700 Ci/mmol in a synthesis time of 1.5 h. The in vivo biodistribution results will be presented.

^{18}F-Ph-CH_2-N(CH_3)CH_2C≡CH (1)

^{18}F-Ph-CH_2-NHCH_2C≡CH (2)

Posterboard 1162

COMPARATIVE BLOOD BRAIN BARRIER TRANSPORT OF 6-[F-18]FLUORO-L-DOPA AND REGIOSPECIFICALLY LABELED L-[C-14]DOPA. D.W. Cheng, N. Satyamurthy, W.H. Oldendorf, J.R. Barrio, and M.E. Phelps. UCLA School of Medicine, Los Angeles, CA.

Using Oldendorf's brain uptake index (BUI) technique (W.H. Oldendorf, Brain Res. 24:372-376, 1970), 6-[F-18]fluoro-L-DOPA (FDOPA) transport was studied at the blood brain barrier (BBB) in rats. Appropriately labeled L-DOPA and [H-3]H_2O in Ringer solution (pH 7.40) were injected into the common carotid artery (0.2 ml bolus) using a 27-gauge needle syringe. To evaluate the effect of brain endothelial aromatic amino acid decarboxylase (AAAD) on transport, control rats were compared with rats treated with L-α-methyldopa hydrazine (carbidopa; CD)(50mg/kg s.c., 60 min. before injection). To minimize further metabolism by intraneuronal AAAD, rats were sacrificed by microwaving. The cerebral BUI values in control rats were 23.6±2.3 (n=3) and 33.4±9.3 (n=4) for L-1-[C-14]DOPA and L-3-[C-14]DOPA, respectively. Differences are due to AAAD mediated capillary decarboxylation, that produces [C-14]O_2 losses with the former. This was confirmed because in the presence of CD, similar BUI values were obtained for L-1-[C-14]DOPA (37.2 ± 9.0, n=3) and L-3-[C-14]DOPA (41.1±8.7, n=4). The effect of intraneuronal AAAD activity during tissue processing was observed in rats which were decapitated instead of microwaved. For example, cerebral BUI values for L-1-[C-14]DOPA in the presence of CD were 37.2±9.0 (n=3) by microwaving versus 21.7±1.6 (n=3) when animals were sacrificed by decapitation. FDOPA to L-3-[C-14]DOPA uptake ratios were 1.15±.09 (n=3) and 1.14±.15 (n=3) for the cerebrum and cerebellum, respectively. In CD treated rats, the same ratios were observed (1.14±.08 (n=3) and 1.32±.07 (n=3), respectively). Therefore, in rats, FDOPA has transport characteristics similar to L-DOPA, with a higher BBB permeability (14%±8%). Moreover, the results with L-DOPA indicate that FDOPA would likely be decarboxylated at the brain capillaries in the absence of CD, decreasing the amount available for neuronal conversion to 6-[F-18]fluorodopamine.

Posterboard 1163

SYNTHESIS OF β-[F-18]FLUOROMETHYLENE-m-TYROSINE DERIVATIVES, A DUAL-ENZYME ACTIVATED INHIBITORS OF MONOAMINE OXIDASE. G.N. Reddy, N. Satyamurthy, J.R. Barrio, and M.E. Phelps. UCLA School of Medicine, Los Angeles, CA.

β-Fluoromethylene phenethylamine derivatives are potent, enzyme-activated, and irreversible inhibitors of Type B monoamine oxidase (MAO). These compounds originate in-vivo by decarboxylation of phenylalanine precursors by aromatic amino acid decarboxylase, predominantly located in brain in monoamine nerve endings. The title compounds would thus be dual enzyme activated markers for a very selective in-vivo assessment of MAO localization and function in catecholamine nerve terminals. The present study describes the synthesis of such F-18 labeled fluoromethylene-m-tyrosine derivatives. Two approaches for F-18 labeling are described herewith: a) when m-methoxyacetophenone was condensed with ethyl isocyanoacetate, followed by acid treatment, the E/Z isomers of ethyl α-formylamino-β-(3-methoxyphenyl)-β-methyl propenoic acid were obtained. The dianion of this, when quenched with F-18 labeled acetyl hypofluorite (AcOF) or elemental fluorine gave ethyl β-fluoromethyl-α-formylamino-β-(3-methoxyphenyl) propenoic acid in modest yields (H-1 NMR-CH_2F, 5.92, d, 47 Hz; F-19 NMR -CH_2F, -215.3 ppm), a reaction hitherto of no precedence. Reported isomerization and hydrolysis afforded β-[F-18]fluoromethylene-m-tyrosine. b) Alternatively, F-18 label was introduced in the phenyl ring of the target compound. Condensation of α-fluoro-3-methoxyacetophenone with hippuric acid in the presence of lead tetraacetate gave E/Z isomers of 4-[(3-methoxyphenyl) fluoroethylidene]-2-phenyl-5(4H)-oxazolone which was radiofluorinated with F-18 labeled F_2 or AcOF. The ratio of the fluorinated 2,4 and 6 regioisomers formed was found to be a function of the polarity of the solvent in various solvents. Thus, fluorination of the above oxazolone with [F-18]AcOF in acetonitrile gave predominantly 4-[(4-fluoro-3-methoxyphenyl) fluoroethylidene]-2-phenyl-5(4H)-oxazolone. Deconjugation of the double bond with lithium diisopropylamide, followed by acid hydrolysis, afforded the desired 4-[F-18]fluoro-β-fluoromethylene-m-tyrosine.